A Unified Law of Mortality for Economic Analysis

Adriana Lleras-Muney and Flavien Moreau*

August 20, 2019

Abstract

We propose a dynamic production function of health and use it to understand the dynamics of population mortality and health from birth to death, across time, and across species. Our parsimonious model provides an excellent fit for the mortality and survival curves for both primate and human populations. The model sheds light on the dynamics behind many phenoma documented in the literature, including (i) the existence and evolution of mortality gradients across socio-economic statuses, (ii) non-monotomic dynamic effects of in-utero shocks, (iii) persistent or "scarring" effects of wars and (iv) mortality displacement after large temporary shocks such as extreme weather.

JEL: I10, J11

Keywords: Mortality, Health, In-utero shocks, Selection, Scarring.

Health and longevity are key determinants of economic activity, affecting fertility, productivity, human capital investments, savings, and retirement decisions. In turn many economic factors and policies have important effects on a population's health and mortality. Yet, we lack a coherent framework to understand how population health and mortality evolve over the lifetime, and how economic and other environmental factors affect this evolution. In the absence of a quantitative model of the lifelong evolution of health and mortality it is difficult to predict how shocks will affect population health at various ages, and even harder to design optimal investment or compensation policies (Almond et al., 2018).

This paper provides a simple dynamic model of the production of health and mortality from birth to death for a heterogenous population living in a stationary economic environment. Because the model tracks individuals' health and mortality throughout the lifetime, it can be used to analyze demographic responses to changes in the socio-economic environment. We estimate this model and show that it is consistent with the following stylized facts: (1) the profile of log mortality rates by age has a tick-mark shape in most species, and (2) survival curves for humans have "rectangularized" over the last two centuries. We then show that simple extensions of this model can be used to rationalize various well-documented mortality phenomena, including (3) persistent gaps in mortality rates across populations with different socio-economic status that fall with age (aka "SES gradients"); (4) non-monotonic health impacts of in-utero shocks over the lifetime; (5) scarring effects of short-term negative shocks such as wars; and (6) "harvesting" or mortality displacement after temporary changes in environmental conditions.

The evolution of mortality over the lifetime is remarkably similar across human and primate populations. The logarithm of mortality has the shape of a "tick mark": high at birth, low among the young, and high and rising almost linearly with age in late adulthood. This is shown in Figure 1 for human females. The figure plots the logarithm of mortality rates by age, for selected birth cohorts of women born between 1860 and 1940 of various European countries (panel a) and for France (panel b).

Because of this consistency demographers have searched for a "unified" model of mortality at least since the early 19th century (Gompertz, 1825). Like much of the following literature (e.g. Li and Anderson, 2013) Gompertz's model only accounts for mortality *after a certain age* – typically after age 30-40. There are a few exceptions. An early model proposed by Heligman and Pollard (1980) uses 8 parameters to describe the probability of dying at a given age for all ages. More recently Sharrow and Anderson (2016) and Palloni and Beltrán-Sánchez (2016) propose alternative models of survival rates that also fit survival curves well. Our approach differs in one fundamental aspect from these. As in the seminal Grossman (1972) model, we model how the health stock of individuals evolve, rather than directly modeling the mortality or survival rates of the population.

In the spirit of classic demographic work (Vaupel et al., 1979), the model assumes that some individuals are born more frail than others and tend to die young. Subsequently, the health distribution of the survivors evolves according to a simple law of motion that depends on the level of external resources and their distribution.[1] As in Grossman (1972), the health stock deteriorates with age but can increase if (health) resources are invested. But unlike Grossman (1972), resources in our model are stochastic, a crucial distinction. In addition, individuals can die from accidents unrelated to their health status. These "external" causes of death play an important role in explaining the level of mortality during the adolescent years.

We use high quality data from the Human Mortality Database to estimate the model and to show that it provides an excellent characterization of the age-profiles of mortality for cohorts born in the early 19th century and later.[2] We focus on French women mainly for two reasons: the French data go back in time

---

[1] The model can be seen as formally similar to the stochastic processes used to model corporate defaults (Lando, 2004).

[2] The HMD has some important limitations. Migration is not accounted for. Counts are not accurate for years during which the

Figure 1: Mortality rates across populations
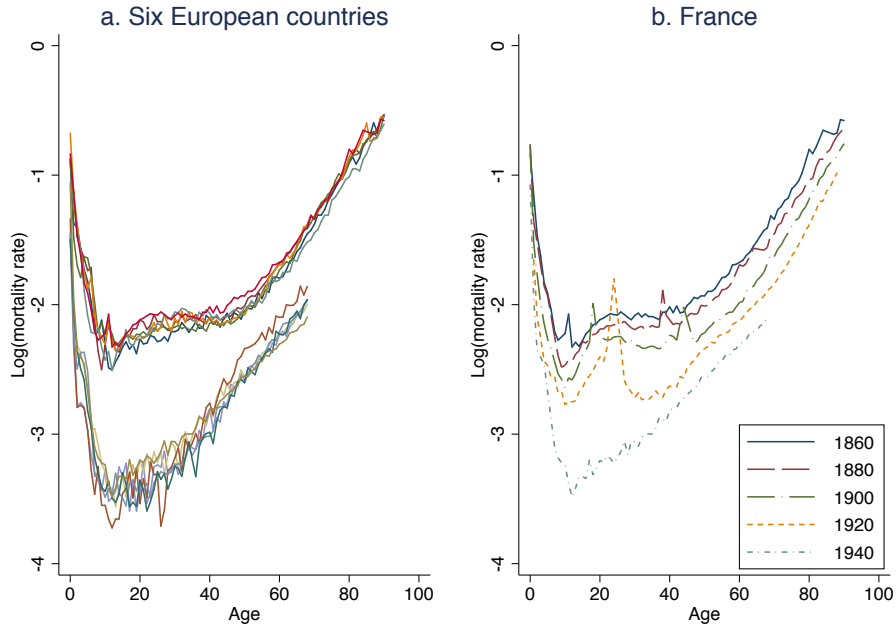
Note: Human Mortality Database. *Panel a* shows the $\log_{10}$ of the mortality rates by age for women born in 1860 and in 1940, in six European countries (Belgium, Denmark, the Netherlands, Sweden, France, and Norway). *Panel b* shows the mortality rates for women born in France in 1860, 1880, 1900, 1920 and 1940.

to 1816 and cover a large population.[3] The Human Mortality Database provides population and death counts by age, birth-year and gender collected through vital registration systems (birth and death certificates) and censuses, from 1816 up to 2015. We compute mortality rates by age for each cohort as the number of deaths divided by the population at that age, and use these to compute survival rates.[4] We then use the simulated method of moments to estimate model parameters, and conduct counterfactual exercises.

Our approach is better suited for the study of causal mechanisms than the demographic approach. We can characterize how factors at a given age affect health and mortality at later ages because we model inputs into health directly and trace their effects. For instance, we study the effects of increasing lifetime resources or the impact of negative in-utero shocks on a population's average health and mortality. We also demonstrate that the model can be used to track the effects of temporary shocks such as WWII or droughts. In addition to providing a parsimonious model that traces health from birth to death, this framework can be used to think about the level and timing of optimal investments or compensatory investments.

To our knowledge there is no other model that can accurately predict the lifetime health of a population, while providing a law of motion for health at the individual level. Because we track populations we can

---

territory changed, in 1861, 1869, 1914, 1920, 1939, 1943, 1945, 1946 – often corresponding to wars (see Appendix 4). Data is imputed for ages above 90.

[3]Most studies of health and mortality investigate men and women separately. An analysis of gender differences is beyond the scope of this paper.

[4]Technically, we compute annual probabilities of dying at a given age. Since the HMD provides no information on the distribution of births and deaths *within* a year, we make no adjustments for the fact that the deaths in the first year do not correspond to individuals born that year. The HMD reports probabilities (q_x) that make adjustments based on a series of standard assumptions in epidemiology and demography. In order to avoid introducing discrepancies, we treat the data and the model symmetrically by computing death probabilities naively. These probabilities are very similar to the ones HMD computes (See Appendix Figure 6).

make predictions about mortality rates, selection, and about the average health of the survivors. No paper that we know of has made use of the age-profile of mortality over the entire lifetime of a cohort to make inferences about the evolution of health and estimate counterfactuals. Our model is both realistic and very rich in its predictions. However we do not attempt to model utility or optimal resource allocation: the absence of cohort data on incomes, health inputs, and their prices over time limits our ability to empirically estimate a richer model. On these dimensions, our model is much simpler than the original Grossman model, or more recent and sophisticated versions of the Grossman model by Dalgaard and Strulik (2014) or Galama and Van Kippersluis (2018). Our contribution is to identify a parsimonious but realistic parametric model of the dynamic production of health and mortality, upon which more complex but realistic models can be built.

1   A Unified Model of Aging and of "Natural" Mortality

Individuals are born with an initial health endowment H_0. This initial health endowment differs across individuals in the population and has an unknown distribution. Every period the environment provides resources I to all individuals, which increase H. In addition, individuals in the environment are more or less lucky, and experience an idiosyncratic shock ε_t to their resources. For example I characterizes the per capita amount of food that a country produces, but a given person might receive less if for instance rain was unusually low in their location. The variance of ε_t captures how unequal the distribution of resources within the population is. These idiosyncratic shocks are assumed to be i.i.d. every period. Finally, the health stock depreciates each period by an amount $d(t)$, which is increasing in t $(d'(t) > 0)$: every period there is a "user cost", reflecting cumulative cell death and organ damage. Together these forces determine the evolution of the health stock, which is an unobserved latent variable.

Individuals die when their stock of health dips below a threshold $\underline{H}$, which is fixed throughout the lifetime and identical for all individuals. Let $D_t = \mathbb{I}(H_t \leq \underline{H}, D_{t-1} = 0)$ denote the random variable equal to one if the individual dies in period t. The population's health and mortality is characterized by the following dynamic system:

$$\begin{cases} H_t = H_{t-1} - d(t) + I + \varepsilon_t & \text{if } D_{t-1} = 0 \\ D_t = \mathbb{I}(H_t < \underline{H}, D_{t-1} = 0), \\ D_0 = 0 \end{cases}$$

with $I \in \mathbb{R}$. Note that if $D_t = 1$ then H_t is undefined – we do not observe the health of individuals after they die. But we observe the mortality rate for the population at time t which is given by $MR_t = P(D_t = 1|D_{t-s} = 0 \forall s < t)$. Thus the distribution of health at any age is a function of the entire history of shocks and investments, as can be seen from the definition of MR_t, which conditions on survival in every previous period.

In order to make the model more tractable, we make three parametric assumptions. First, H_0 follows a normal distribution $\mathcal{N}(\mu_H, \sigma_H^2)$. This is an arbitrary assumption, although one that is consistent with indirect evidence: for instance the empirical distribution of birth weights is normal (Wilcox and T Russell, 1983). Second, shocks to resources every period also follow a normal distribution $\varepsilon_t \sim \mathcal{N}(0, \sigma_\varepsilon^2)$.[5] Third,

---

[5]Conceptually the model has no difficulty accommodating other distributions. But simulations with alternative assumptions (e.g. log normal errors) resulted in counterfactual mortality rates and a poorer overall fit.

depreciation is a power function $d(t) = \delta t^\alpha$ with $\delta \in (0, \infty), \alpha \in (0, \infty)$.[6] The aging process in the model starts directly at birth, consistent with evidence that aging markers are evolving among children (Wong et al., 2010) and increases with age, as in biological models of senescence (Armitage and Doll, 1954; Pompei and Wilson, 2002).[7]

Initially, the health distribution is normal. Then the health distribution shifts to the right during the first period (as long as I is positive and larger than the aging term) and spreads out (because of the stochastic shock ε_t). Individuals who were born too frail or who experience large negative shocks move to the left of the threshold and die. Graphically, the infant mortality rate (the fraction of individuals that die in the first period) corresponds to the area under the curve below the threshold (see Appendix Figure 7). In the second period, this truncated distribution moves right again (if I is large relative to $d(1)$).[8] And the population receives a new shock, generating mortality again among those with large negative shocks. This illustrates the importance of the stochastic term ε_t. In its absence, there would be no deaths in period 2 – nor in any subsequent period, until the depreciation term becomes large enough to push the leftmost part of the distribution below the threshold. Then mortality increases every period.[9] The evolution of the health distribution and the resulting mortality are shown in Appendix Figure 8b.

External causes of death. Not all deaths have direct biological causes. In fact, many deaths, like accidents or homicides, strike individuals regardless of their health status. These "extrinsic" causes of death can be integrated in the model by simply adding an i.i.d. "accident shock" that is independent of the stock of health H_t.[10] Then a constant fraction $\kappa \in [0, 1]$ of the population is randomly killed every period.[11] This model does not change the basic properties of the model. (Log) Mortality rates simply increase at all ages as a result – though more so for young adults. See Appendix Figure 9.

Contemporary data however show that the mortality rate from external causes of death is not constant throughout life, and instead is well approximated by a step function, with a major increase around adolescence (see Appendix Figure 10). Hormonal, marital, consumption and work patterns change substantially during adolescence. These disruptions are thought to manifest themselves on the mortality curves as an "adolescent hump," especially visible in cohorts born in the 19th century (Preston et al. 2000; Thiele, 1871). Based on this evidence, we assume that κ starts as zero but becomes positive in adolescence.

Estimation. The model characterizes the biological evolution of health and mortality of a cohort using 6 (rescaled) parameters: one for the mean initial health (μ_0), two governing the aging process (δ, α), two characterizing the effects of resources, in the form of average investments (I) and the variance of these investments or shocks (σ_ε^2), and one (κ) capturing the accident rate increase occurring in adolescence.[12]

---

[6]Our estimates for human populations find that $\alpha > 1$ and the depreciation is therefore convex in age, as hypothesized by Grossman. This is not imposed *a priori* by the model.

[7]See Gavrilov and Gavrilova (1991) and Weibull (1951) for attempts at biological micro-foundations drawing on reliability theory from engineering.

[8]If, in the first period, depreciation were very large relative to investment, then mortality would rise from birth onwards – a theoretical possibility observed neither among humans nor primates.

[9]If I is less than aging then one could also generate positive mortality in the second period without a stochastic term but then mortality would be rising from age 2 onwards, which we do not observe in the data.

[10]Corporate default models similarly complement the equation describing the evolution of firms' values with a "jump to default" component.

[11]This random accident rate places a floor in the level of mortality that is constant across ages. If all health-related deaths were eliminated, this accident rate would uniquely determine the life expectancy of the population ($1/\kappa$).

[12]Two out of the eight parameters of the model cannot identified. To see this, note that the expression for mortality in the first period (shown in Appendix Figure 7) is the standard Probit model. We can subtract $\underline{H}$ and divide by σ_H on both sides of the expression determining the probability of dying, and leave the mortality rate unchanged. Therefore the threshold $\underline{H}$ and the standard deviation of the initial distribution σ_H are not identified. Without loss of generality we therefore set $\underline{H} = 0$ and $\sigma_H = 1$. More precisely we need to normalize 2 out of three parameters. We find it more intuitive to normalize the threshold rather than the initial mean, but this choice is arbitrary.

Figure 2: Model fit for humans and primates

(a) French woman born in 1816   (b) Female chimpanzees
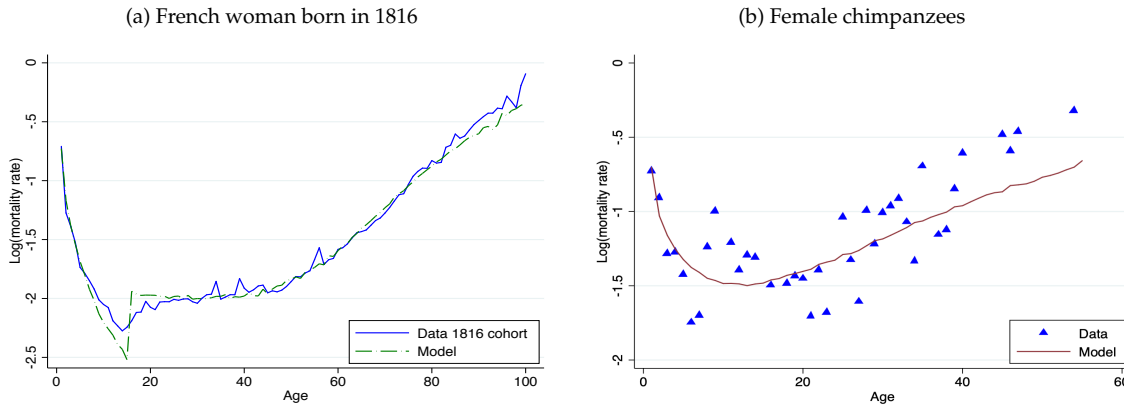
Note: *Panel a* shows the data and estimated curve for French women born in 1816. *Panel b* shows the data and estimated parameters for female chimps. Appendix Tables 1 and 2 show the estimated parameters.

We interpret μ_0 as the distance from the threshold of the initial distribution, in standard deviations of the initial distribution. All other parameters are also expressed in "standard deviation" units, except for α which is "scale free"– it does not depend on the initial distribution. These normalized parameters are identified (see Appendix 4). Despite the model's conceptual simplicity, the mortality rate at a given age cannot be expressed in closed-form.[13] We use a numerical method, the simulated method of moments, to estimate the parameters of the model. Appendix A has the estimation details.

2 Explaining Mortality Patterns

2.1 Mortality rates over the lifetime

Our production function provides an excellent fit for populations in stationary environments.[14] For instance, the model very closely matches the 1816 cohort's mortality rates at every age (Figure 2a). The predicted life expectancy is 38 years and 102 days compared with the actual life expectancy of 38 years and 91 days.[15]

We estimate an initial mean health of about 0.86 so many individuals are born at or below the threshold. Absent any shocks or investment in the first period, infant mortality would have been roughly 15% (instead of 17%). Mortality falls dramatically after age 1 because (1) there is selection (many frail individuals have already died), and (2) investment (estimated as 0.4), is large relative to aging in the first period (δ estimated as 0.0006). This results in a net improvement in mean health and moves the population distribution of health to the right leaving no one below the threshold. But the variance of resources is large (estimated to be roughly 1) so a few unlucky individuals still fall below the death threshold after age 2. So long as I remains high relative to aging, mortality falls.

In adolescence mortality rises sharply in both the data and the model because external causes of death

---

[13]Our discrete model is similar to a class of models used for corporate' default probability and securities pricing. This literature has established that, except for the particular case of a constant or linear drift, these models do not admit closed-form solutions (see Lando, 2004).

[14]The 1816-1860 cohorts are stationary, their cohort and period mortality curves are almost identical whereas they diverge subtantially in 1940, see Appendix Figure 11.

[15]Appendix Table 1 shows alternative measures of fit and the estimated parameters.

increase.[16] We estimate a mortality rate of roughly 9 per thousand, every year after adolescence starts, lowering the 1816 cohort's life expectancy by about 7.6 years. Log mortality starts rising almost linearly roughly after age 45. This occurs because while δ is small (~ 0.0006) the aging rate α is around 1.8, so that the aging function δt^α is increasing more than linearly with age. Because health resources I are increasing only linearly, eventually all individuals die, even lucky ones with many large positive health shocks.[17]

Human mortality patterns are very similar to those of other primates and therefore our basic model should describe primate mortality as well. We estimate the model using the best available data on populations of female chimpanzees living in the wild from Bronikowski et al. (2011). Because these populations are small, the estimates are much noisier, but we still obtain a very good fit (Figure 1b).

Health. The model has implications for the distribution of health among the living. Because health is unobserved, these implications are not testable. But three pieces of empirical evidence using health proxies are broadly consistent with the model: (1) in the model, mean health rises and then falls with age, peaking in mid-life (Appendix Figure 8b). This behavior is consistent with the evolution of self-reported health by age among adults (Deaton and Paxson, 1998, Case and Deaton, 2005), and with morbidity patterns by age;[18] (2) the variance of health is also predicted to rise and fall. It rises because each per period's shock is normal and not perfectly correlated across individuals. But this variance falls late in life because of mortality. This is what Deaton and Paxson, 1998 observe; (3) at any given age after infancy and before old age, the distribution of health is roughly gaussian despite repeated truncations, because it is approximately equal to a sum of normal distributions. This is consistent with the observation that health measures like heights, which evolve until adulthood, are close to normally distributed.[19]

2.2 Rectangularization of the Survival Curves

Remarkably, the model's performance extends to non-stationary environments and it is able to track the evolution of the mortality profiles over all the successive cohorts since 1816. This evolution is characterized by a "rectangularization" of the survival curves, that has accelerated over the last decades. Panel a in Figure 3 shows the rectangularization of the survival curves of French women born between 1816 and 1947. Survival to age 1 has increased dramatically. The next section of the survival curve – roughly from age 1 to age 60 – has considerably flattened. In addition, a steep downward slope has emerged among the oldest. As a result, more than 70% of those born in 1940 live past age 70, whereas in the 1816 cohort fewer than 30% did.[20] Panel a in Figure 3 shows that the model captures this rectangularization with great accuracy. The model can fit the data for the 1940 cohort almost as well as for the 1816 cohort.

---

[16]We assume adolescence starts at age 16, based on historical estimates from de La Rochebrochard (2000) who reports that the onset of menarche occurred around 15.8 in 1816. We have estimated models where the onset of adolescence is a parameter and obtained similar results (see Appendix Table 3). Conceptualizing the adolescent hump as a permanent change in another parameter of the model results in subtantially worse fit in the data (See Appendix table 1)

[17]See Appendix 4 for a rigorous proof.

[18]The model generates morbidity rates that are a U-shaped function of age (where morbidity rate is the fraction of individuals with health below a health threshold but above the death threshold). Contemporary data show that hospitalization days (a proxy for morbidity) are indeed U-shaped (see table P-10 in Centers for Disease Control and Prevention 2014).

[19]For example Limpert et al. (2001) show that either a normal or a log normal distribution fits female heights well.

[20]This corresponds to log mortality curves which have been shifting down in roughly parallel fashion as shown in Appendix 12.

Figure 3: Evolution of survival for French females born 1816-1940

(a) Observed and Estimated Cohort Survival Rates   (b) Parameter evolution
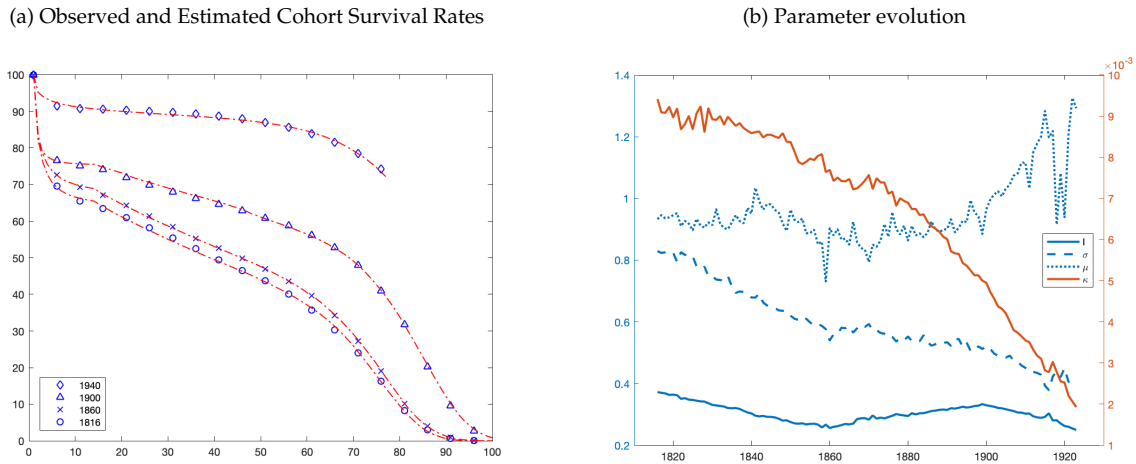
Note: *Panel a* shows the observed (blue markers) and estimated (red dashes) survival curves for four cohorts of French women born about 40 years apart between 1816 to 1923. *Panel b* displays the evolution of estimated parameters, except for the aging parameters which are shown in Appendix Figure 13. On the left axis are the values for the three blue lines corresponding to resources (I), the variance of the lifelong shock (σ), and initial health at birth (μ). The accident rate κ in red is on the right axis. The model is estimated separately on each cohort treating the two World War as two independent negative resources shocks, see Appendix C for details.

Cohort life expectancy rose from 40 for the 1816 cohort, and to about 69 for the 1923 cohort (the last cohort that is almost extinct). What are the sources of these increases in longevity? Panel b in Figure 3 shows the evolution of four of the estimated parameters from 1816 and 1923. Starting in the 1830s we see a constant and rather drastic decline in external causes of death, which is consistent with the elimination of maternal mortality (a major cause cause of death among prime-age women in the past), and with the steep decline in violent deaths documented for instance by Pinker (2011). Health at birth, μ_0, started to increase steadily only at the turn of the century, consistent with the timing of improvements in water, sanitation, and the elimination of epidemic and infectious disease mortality, which greatly reduced infant mortality (Cutler et al., 2006). By contrast health resources (I) did not change much in the 19th century (they fall a bit and rise again) consistent with the debate on the questionable benefits of the Industrial Revolution on living standards.

More surprisingly, we also observe a substantial decrease in the force of aging (shown in Appendix Figure 13), the causes of which are unclear. Since food consumption and heights were rising, this suggests that nutrition is a possible determinant of the aging function (Fogel, 1994). Finally there is a steady decline in the variance of health resources – it is also unclear why this occurred though it is possible food availability became less variable. More evidence is needed to understand these trends.

3   Understanding Mortality Dynamics

The evolution of the parameter estimates for each cohort suggests large, lasting changes in the environment. In this section, we investigate how environmental changes and their implications on mortality rates can be understood, through the lens of the model, as proceeding from simple shocks to one or several parameters.

3.1 Socio-Economic Status Mortality Gradient

A substantial literature documents health and mortality "gradients" – large and persistent differences across individuals with different levels of socio-economic status such as education, income level, occupation or race (Cutler et al., 2012). For instance, Americans with a high permanent income level at age 40 have lower subsequent mortality relative to those with lower incomes (Chetty et al. 2016). Figure 4a reproduces Chetty et al. (2016)'s figure showing that the log mortality curves partly converge in old age (implying smaller gaps at older ages in percentage terms).

Suppose that we extend our model so that lower income leads to lower I throughout life.[21] We simulate the effect of lowering I by 50% on the 1816 French cohort to investigate the consequences. Figure 4b shows this results in higher and flatter log-mortality curves for the poorer population. The curves for the rich and the poor converge in old age, just as documented by Chetty et al. (2016). Similarly, more educated individuals tend to have healthier behaviors (Cutler and Lleras-Muney 2010). If education leads to greater I, we would observe a similar pattern with the log mortality rates of the educated being lower and steeper than those of the less educated, and the gap between would narrow with age. This exactly matches what the literature has found: in their review Hummer and Lariscy (2011) write "analyses invariably show that educational disparities in mortality are narrower at older than at younger adult ages."

This narrowing of the mortality SES gradient (in percentage terms) occurs in the model only *after a certain age*.[22] As Appendix Figure 14 shows, the effect of greater I on mortality initially grows with age, as hypothesized by the cumulative advantage hypothesis (Lynch 2003, Ross and Wu 1995), because greater I pushes the entire population further and further away from the threshold every period. However gradients eventually fall because of selection, as suggested by Crimmins (2005): the population with lower I starts dying, leaving only the healthiest individuals alive.

Lastly the figure also shows that in *levels*, SES gaps in mortality rates are u-shaped instead of hump-shaped with age. Thus they are very small among prime adults, and possibly hard to detect in finite samples, but they rise with age as Kaestner et al. (2018) show for education.
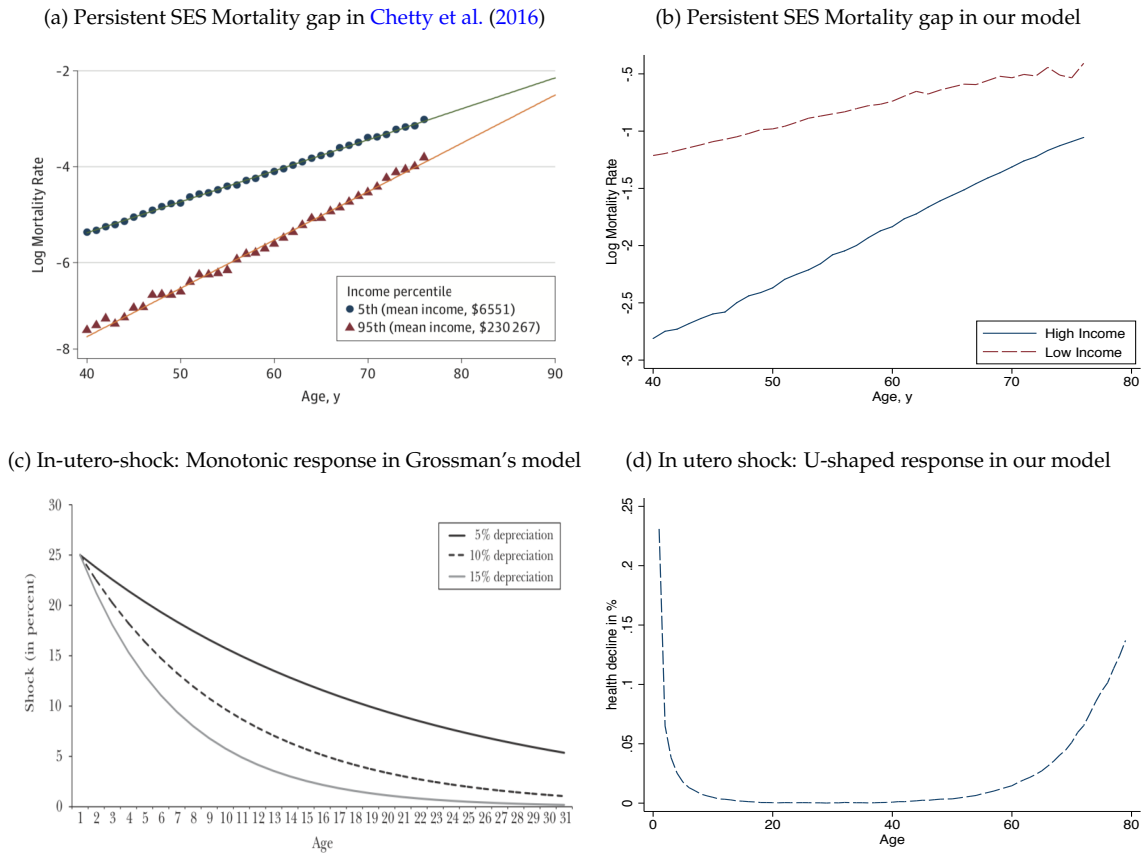
Health. Lower income and thus lower I is also predicted to lower average health at all ages. But the effect increases with age, and then declines once mortality starts rising (in both levels and percentage terms. (See Appendix Figure 14.) These predictions match the evidence in Case et al. (2002), Currie and Stabile (2003) and House et al. (2005), who show that the gaps in self-reported health status and morbidity between those born in poor and rich families grow with age, but decline after 65.

Resources or depreciation? Higher SES could lower rates of aging, for instance due to more frequent physical exercise, lower exposure to pollution or lower stress. In the model an increase in the aging parameters (δ or α) and a decrease in I generate similar health and mortality profiles among the old (see Appendix Figure 15). Thus, with data from (mature) adults *only*, it is not possible to infer whether SES is affecting annual resources I or the aging rates. But higher aging rates do not result in any visible health or mortality gaps among children, whereas higher I does. Therefore the evidence in Case et al. (2002) or Currie and Stabile (2003) interpreted through the lens of the model, suggests that changing family income is equivalent to changing I. It is possible to break this observational equivalence by using measures of aging. Liu et al. 2019 find that education and race are associated with lower methylation rates, suggesting SES also affects aging.

---

[21]In other words, assume there is a function $I = I(Y, E)$ with $I' > 0$ for all inputs such as income Y or education E.

[22]Note that the gap in *levels* between the high and low I populations is hump shaped with age instead of U-shaped, growing with age among older adults (Appendix Figure 14).

Figure 4: Contrasted dynamics: SES gradients vs. in-utero shocks

(a) Persistent SES Mortality gap in Chetty et al. (2016)

(b) Persistent SES Mortality gap in our model

(c) In-utero-shock: Monotonic response in Grossman's model

(d) In utero shock: U-shaped response in our model

Note: *Panel a* reproduces the results from Chetty et al. (2016). *Panel b* shows the predicted mortality rate for the 1816 cohort (using the parameters from in Appendix Table 1 but setting the accident rate at 0 throughout for simplicity) and the counterfactual mortality that results from a 95% decline in I for this population. The baseline 1816 cohort is labeled "High Income" and the counterfactual population is labeled "Low Income." *Panel c* is reproduced from Almond and Currie (2011) and shows the decline in the health stock due to a shock in utero that is predicted by the standard Grossman model. This effect is initially large but it fades over time and will be close to zero among adults older than 30. *Panel d* shows the simulated effects of a 50% decline in in-utero health for the 1816 French population in the model (setting the accident rate at 0 throughout for simplicity).

3.2 Non-Monotonic Effects of In-Utero Shocks

Detrimental events in-utero (famines, war, stress) result in large and persistent declines in health that are visible in infancy and old age (Almond and Currie, 2011). Surprisingly, the effects of various shocks appear to "fade out" initially, only to re-appear later in life. (See Almond et al. (2018) 's comprehensive review.) They point out that while the initial fading out is consistent with the canonical Grossman (1972) model, the non-monotonicity of the effect is not. The Grossman model predicts a large immediate decline in the population's health after an in-utero shock that becomes hardly visible in adulthood (Figure 4c).

Our model, by contrast, predicts exactly the U-shaped pattern noticed by Almond et al. (2018). Figure 4d documents that lowering initial health μ by 50% for the 1816 French cohort results in lower health among the survivors at all ages – both in levels and in percentages – with a u-shaped pattern with age. This occurs without complementary or compensating investments. The reason this happens in our model (but not in Grossman's) is that depreciation in our model is not multiplicative in the stock. These results suggest it is not possible to identify the effects of in-utero shocks with health data for on adolescents or young adults only. Schiman et al. (2017), who study the effects of experiencing WWII in utero and early childhood, find that its effects on health, disability, and employment among adults are not visible for young adults, but grow with age, as predicted.

Interestingly, the predicted effects of negative in-utero shocks on mortality fall with age (in percentage terms though not in levels, see Appendix Figure 16) though this pattern is not necessarily monotonic: in middle ages when mortality levels are low, the effects can rise and fall due to small samples. Future work should further investigate these predictions.

In the model initial endowments and investments are complements in the health production function. The same is true of early and late investments, which exhibit dynamic complementarity, as in Cunha and Heckman (2007). (See Appendix A.) This has important implications for compensatory investments.
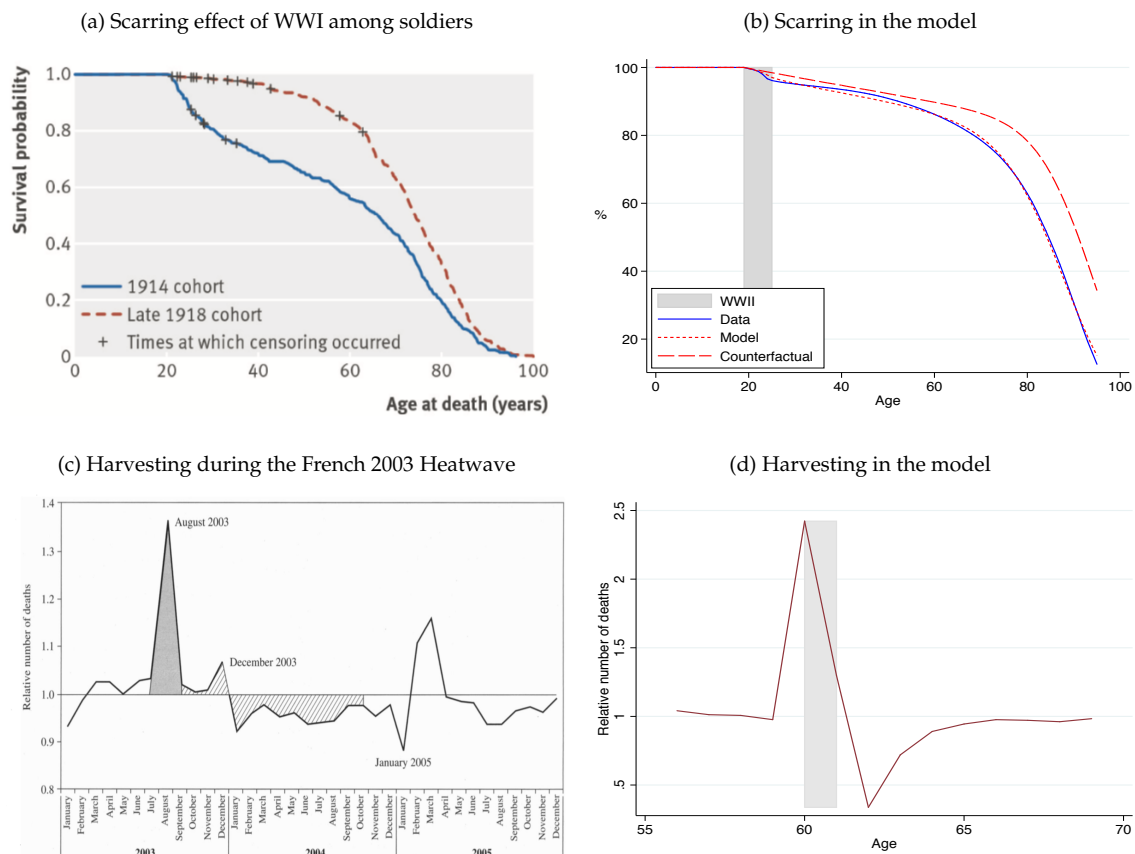
3.3 Scarring Effects of Wars

Wars have long-lasting detrimental health effects among survivors. Such "scarring" effects have been documented in at least 13 European countries after WWII. Compared to less exposed survivors, individuals who were more exposed to the war experienced worse economic and health outcomes several decades later (e.g. Kesternich et al., 2014, Havari and Peracchi, 2017).[23] Figure 5a Panel a (reproduced from Wilson et al. 2014) shows the scarring of World War I on New Zealand military personnel.

The model can successfully reproduce this scarring effect when the war is modeled as a temporary decrease in I. Figure 5b shows the mortality curve obtained from estimating a model with a 6-year change in I at age 18 for the 1921 cohort (corresponding to WWII), and simulating the counterfactual curve if the I-shock due to the war is shut off.[24] The model predicts what Wilson et al. (2014) observe in the data: the survival curve for the affected cohort is lower than the survival curve for the unaffected cohort, during the war and thereafter. Our patterns are somewhat different because we estimate the model for a population of French women (instead of New Zealand soldiers), who suffer many fewer deaths during wars. But the results show that the model generates scarring. We estimate that war lowered life expectancy by approximately 5 years for the 1921 cohort. Conditional on surviving to 1945, life expectancy is also 5 years lower

---

[23]Costa (2012) documents scarring effects of the American Civil War on surviving soldiers.

[24]This assumption is consistent with historical data for WWII. GDP declined substantially during the war and 20 to 55% of it was appropriated by Germans during the occupation (Occhino et al., 2007). Food rationing began in 1940. We can assume that the war is a different type of shock. Appendix Table 4 shows that an I-shock predicts the number of deaths during the war best.

Figure 5: Generating scarring and harvesting

(a) Scarring effect of WWI among soldiers

(b) Scarring in the model

(c) Harvesting during the French 2003 Heatwave

(d) Harvesting in the model

Note: *Panel a* is from Wilson et al. (2014) and shows the scarring effect of WWI. It compares the survival curve of the cohort of young New Zealand military personnel who left for the war in 1914, with the cohort who left for the war in 1918 but did not see active combat. The median age in the sample is 24. *Panel b* shows the scarring effect of WWII for women born in France in 1921 who turned 18 when WWII started in 1939. It allows for I to be different from 1939 to 1945. Instead of using a comparison group, the model is used to compute the counterfactual curve. *Panel c* is from Toulemon and Barbieri (2008) and shows the mortality displacement created by the French 2003 Heatwave. The number of excess deaths in Summer 2003 is computed relative to the number of deaths during the same period in 2000. The grey and (resp. hatched) area correspond to an excess (resp. deficit) of 15,000 deaths. These excess deaths are computed for the entire population. *Panel d* shows the simulated effects of a temporary increase in the threshold at ages 60 and 61 on the 1816 French cohort (setting the accident rate to 0 for simplicity) which results in approximately 8000 excess deaths during the shock and fewer deaths for the subsequent 10 years.

than it would have been in the absence of the war.[25]

3.4 Harvesting Effects or Mortality Displacement

Extreme weather or pollution events appear to displace the distribution of deaths in the short term, creating a sudden increase in the number of death followed by abnormally low mortality. In demography this phenomenon is known as "harvesting" and has been, for instance, documented in France during the 2003 heatwave (see Figure 5c).[26]

A change in the death threshold generates harvesting in the model, and does so by killing the least healthy.[27] Suppose that the death threshold $\underline{H}$ is mostly a function of the environment and technology. Two equally healthy populations will exhibit different death rates if the environment they live in is different. The weather is an example of an environmental factor that can affect survival rates.

Figure 5d shows the simulated effect of a temporary increase in the threshold at ages 60 and 61 on the mortality of the 1816 cohort. It results in very high mortality during the shock. But mortality starts dropping before the shock ends because the frailest individuals have already died in the first period of the shock, so later on only those that receive a large negative idiosyncratic shock die. Once the weather disruption ends, and the threshold is restored to its original (lower) level, mortality falls substantially because there are very few individuals close to the new (lower) threshold. This holds true for a long time until the aging process naturally lowers health stocks again, closer to the new lower threshold.

4 Conclusion

This paper proposes a parsimonious production function to study the evolution of health and mortality over the life course of a population. The basic model has 8 parameters and can be easily estimated by using observed cohort mortality rates. Despite its simplicity, this model tracks the evolution of the mortality profile of human cohorts born 1816 to 1940 as well as other species, and it can explain many important mortality patterns documented in the literature, including rectangularization and SES gradients. We also show how to use the model to understand the dynamic treatment effects of in-utero shocks and other temporary and permanent shocks.

This paper has a few limitations. We make strong parametric assumptions. Health shocks are assumed to be i.i.d and normally distributed. Alternative assumptions for this distribution of annual shocks should also be further investigated. We also assume the environment is stationary and exogenously provides as constant level of resources. This is reasonable for primates or early human populations living in stable environments with few technologies, but not for contemporary human populations.

There are interesting implications to be explored. Preliminary work suggests optimal health expenditures are U-shaped over the lifetime in this model. With systematic data on health inputs, prices and budgets over the life course, these implications would be worth further investigating. The model can be used to investigate other interesting questions such as the origins of gender or cross-country differences. We leave these to future research.

---

[25]There results have limitations. Population and death counts are subject to measurement error during wars because of changes in territory and migration. We assume that a constant decline in resources that started in 1939 and ended in 1945 but rationing continued until 1949, and not all war years were equally difficult. WWII could have also affected other parameters.

[26]For instance see Schwartz (2000) or Zeger et al. (1999)for the effects of pollution, and Deschenes and Moretti (2009) or Deschênes and Greenstone (2011) for the effects of very hot or very cold weather.

[27]Only changes in the threshold generate harvesting in our model (See Appendix Figure 17).

References

Almond, Douglas and Janet Currie, "Killing me softly: The fetal origins hypothesis," *The Journal of Economic Perspectives*, 2011, *25* (3), 153–172.

_ , _ , **and Valentina Duque**, "Childhood circumstances and adult outcomes: Act II," *Journal of Economic Literature*, 2018, *56* (4), 1360–1446.

Armitage, Peter and Richard Doll, "The age distribution of cancer and a multi-stage theory of carcinogenesis," *British journal of cancer*, 1954, *8* (1), 1.

Bronikowski, Anne M., Jeanne Altmann, Diane K. Brockman, Marina Cords, Linda M. Fedigan, Anne Pusey, Tara Stoinski, William F. Morris, Karen B. Strier, and Susan C. Alberts, "Aging in the natural world: comparative data reveal similar mortality patterns across primates," *Science*, 2011, *331* (6022), 1325–1328.

Case, Anne and Angus S Deaton, "Broken down by work and sex: How our health declines," in "Analyses in the Economics of Aging," University of Chicago Press, 2005, pp. 185–212.

_ , **Darren Lubotsky, and Christina Paxson**, "Economic status and health in childhood: The origins of the gradient," *The American Economic Review*, 2002, *92* (5), 1308–1334.

Centers for Disease Control and Prevention, "Summary health statistics: National health interview survey," *Atlanta, GA: Centers for Disease Control and Prevention*, 2014.

Chamberlain, Gary, "Asymptotic efficiency in semi-parametric models with censoring," *journal of Econometrics*, 1986, *32* (2), 189–218.

Chetty, Raj, Michael Stepner, Sarah Abraham, Shelby Lin, Benjamin Scuderi, Nicholas Turner, Augustin Bergeron, and David Cutler, "The association between income and life expectancy in the United States, 2001-2014," *Jama*, 2016, *315* (16), 1750–1766.

Costa, Dora L, "Scarring and mortality selection among Civil War POWs: A long-term mortality, morbidity, and socioeconomic follow-up," *Demography*, 2012, *49* (4), 1185–1206.

Crimmins, Eileen M, "Socioeconomic differentials in mortality and health at the older ages," *Genus*, 2005, pp. 163–176.

Cunha, Flavio and James Heckman, "The Technology of Skill Formation," *The American Economic Review*, 2007, *97* (2), 31–47.

Currie, Janet and Mark Stabile, "Socioeconomic Status and Child Health: Why Is the Relationship Stronger for Older Children?," *The American Economic Review*, 2003, *93* (5), 1813–1823.

Cutler, David, Angus Deaton, and Adriana Lleras-Muney, "The determinants of mortality," *The Journal of Economic Perspectives*, 2006, *20* (3), 97–120.

Cutler, David M., Adriana Lleras-Muney, Tom Vogl, S. Glied, and P. C. Smith, "Socioeconomic Status and Health: Dimensions and Mechanisms.," in "The Oxford Handbook of Health Economics," Oxford University Press, 2012.

Cutler, David M and Adriana Lleras-Muney, "Understanding differences in health behaviors by education," *Journal of health economics*, 2010, *29* (1), 1–28.

Dalgaard, Carl-Johan and Holger Strulik, "Optimal aging and death: understanding the Preston curve," *Journal of the European Economic Association*, 2014, *12* (3), 672–701.

de La Rochebrochard, Elise, "Age at puberty of girls and boys in France: Measurements from a survey on adolescent sexuality," *Population: An English Selection*, 2000, pp. 51–79.

Deaton, Angus S. and Christina H. Paxson, "Aging and inequality in income and health," *The American Economic Review*, 1998, *88* (2), 248–253.

Deschenes, Olivier and Enrico Moretti, "Extreme weather events, mortality, and migration," *The Review of Economics and Statistics*, 2009, *91* (4), 659–681.

Deschênes, Olivier and Michael Greenstone, "Climate change, mortality, and adaptation: Evidence from annual fluctuations in weather in the US," *American Economic Journal: Applied Economics*, 2011, *3* (4), 152–85.

Fogel, Robert W., "Economic Growth, Population Theory, and Physiology: The Bearing of Long-Term Processes on the Making of Economic Policy," *The American Economic Review*, 1994, *84* (3), 369–395.

Galama, Titus J and Hans Van Kippersluis, "A Theory of Socio-economic Disparities in Health over the Life Cycle," *The Economic Journal*, 2018, *129* (617), 338–374.

Gavrilov, Leonid Anatolevich and Natalia Sergeevna Gavrilova, *The biology of life span: a quantitative approach.*, Harwood Academic Publisher New York, 1991.

Gompertz, Benjamin, "On the nature of the function expressive of the law of human mortality, and on a new mode of determining the value of life contingencies," *Philosophical transactions of the Royal Society of London*, 1825, *115*, 513–583.

Grossman, Michael, "On the concept of health capital and the demand for health," *Journal of Political economy*, 1972, *80* (2), 223–255.

Havari, Enkelejda and Franco Peracchi, "Growing up in wartime: Evidence from the era of two world wars," *Economics & Human Biology*, 2017, *25*, 9–32.

Heckman, James, "Varieties of selection bias," *The American Economic Review*, 1990, *80* (2), 313.

Heligman, Larry and John H. Pollard, "The age pattern of mortality," *Journal of the Institute of Actuaries*, 1980, *107* (01), 49–80.

House, James S, Paula M Lantz, and Pamela Herd, "Continuity and change in the social stratification of aging and health over the life course: evidence from a nationally representative longitudinal study from 1986 to 2001/2002 (Americans' Changing Lives Study)," *The Journals of Gerontology Series B: Psychological Sciences and Social Sciences*, 2005, *60* (Special_Issue_2), S15–S26.

Human Mortality Database. University of California, Berkeley (USA), and Max Planck Institute for Demographic Research (Germany). Available at www.mortality.org. Data downloaded in August 2017.

Hummer, Robert A. and Joseph T. Lariscy, "Educational attainment and adult mortality," in "International handbook of adult mortality," Springer, 2011, pp. 241–261.

Ibragimov, I., "On the Composition of Unimodal Distributions," *Theory of Probability & Its Applications*, 1956, *1* (2), 255–260.

Kesternich, Iris, Bettina Siflinger, James P Smith, and Joachim K Winter, "The effects of World War II on economic and health outcomes across Europe," *Review of Economics and Statistics*, 2014, *96* (1), 103–118.

Lando, David, *Credit Risk Modeling: Theory and Applications*, Princeton University Press, 2004.

Li, Ting and James Anderson, "Shaping human mortality patterns through intrinsic and extrinsic vitality processes," *Demographic research*, 2013, *28*, 341–372.

Limpert, Eckhard, Werner A. Stahel, and Markus Abbt, "Log-normal distributions across the sciences: Keys and clues on the charms of statistics, and how mechanical models resembling gambling machines offer a link to a handy way to characterize log-normal distributions, which can provide deeper insight into variability and probability—normal or log-normal: That is the question," *BioScience*, 2001, *51* (5), 341–352.

Liu, Zuyun, Brian H Chen, Themistocles L Assimes, Luigi Ferrucci, Steve Horvath, and Morgan E Levine, "The Role of Epigenetic Aging in Education and Racial/Ethnic Mortality Disparities Among Older US Women," *Psychoneuroendocrinology*, 2019.

Lynch, Scott M, "Cohort and life-course patterns in the relationship between education and health: A hierarchical approach," *Demography*, 2003, *40* (2), 309–331.

Occhino, Filippo, Kim Oosterlinck, and Eugene N White, "How occupied France financed its own exploitation in World War II," *American Economic Review*, 2007, *97* (2), 295–299.

Palloni, Alberto and Hiram Beltrán-Sánchez, "Demographic Consequences of Barker Frailty," in "Dynamic Demographic Analysis," Springer, 2016, pp. 147–176.

Pinker, Steven, *The better angels of our nature: Why violence has declined*, Vol. 75, Viking New York, 2011.

Pompei, Francesco and Richard Wilson, "A quantitative model of cellular senescence influence on cancer and longevity," *Toxicology and industrial health*, 2002, *18* (8), 365–376.

Preston, Samuel, Patrick Heuveline, and Michel Guillot, *Demography: measuring and modeling population processes*, Oxford: Blackwell Publishers, 2000.

Ross, Catherine E and Chia ling Wu, "The links between education and health," *American sociological review*, 1995, pp. 719–745.

Schiman, Jeffrey C, Robert Kaestner, and Anthony T Lo Sasso, "Early Childhood Health Shocks and Adult Wellbeing: Evidence from Wartime Britain," Technical Report, National Bureau of Economic Research 2017.

Schwartz, Joel, "Harvesting and long term exposure effects in the relation between air pollution and mortality," *American journal of epidemiology*, 2000, *151* (5), 440–448.

Sharrow, David J. and James J. Anderson, "Quantifying Intrinsic and Extrinsic Contributions to Human Longevity: Application of a Two-Process Vitality Model to the Human Mortality Database," *Demography*, 2016, *53* (6), 2105–2119.

Thiele, Thorvald Nicolai, "On a mathematical formula to express the rate of mortality throughout the whole of life, tested by a series of observations made use of by the Danish Life Insurance Company of 1871," *Journal of the Institute of Actuaries*, 1871, *16* (5), 313–329.

Toulemon, Laurent and Magali Barbieri, "The mortality impact of the August 2003 heat wave in France: investigating the ?harvesting?effect and other long-term consequences," *Population studies*, 2008, *62* (1), 39–53.

Vaupel, James W., Kenneth G. Manton, and Eric Stallard, "The impact of heterogeneity in individual frailty on the dynamics of mortality," *Demography*, 1979, *16* (3), 439–454.

Weibull, Waloddi, "Wide applicability," *Journal of applied mechanics*, 1951, *103* (730), 293–297.

Wilcox, Allen J. and Ian T Russell, "Birthweight and perinatal mortality: I. On the frequency distribution of birthweight," *International Journal of Epidemiology*, 1983, *12* (3), 314–318.

Wilson, Nick, Christine Clement, Jennifer A Summers, John Bannister, and Glyn Harper, "Mortality of first world war military personnel: comparison of two military cohorts," *Bmj*, 2014, *349*, g7168.

Wong, Chloe Chung Yi, Avshalom Caspi, Benjamin Williams, Ian W Craig, Renate Houts, Antony Ambler, Terrie E Moffitt, and Jonathan Mill, "A longitudinal study of epigenetic variation in twins," *Epigenetics*, 2010, *5* (6), 516–526.

Zeger, Scott L, Francesca Dominici, and Jonathan Samet, "Harvesting-resistant estimates of air pollution effects on mortality," *Epidemiology*, 1999, pp. 171–175.
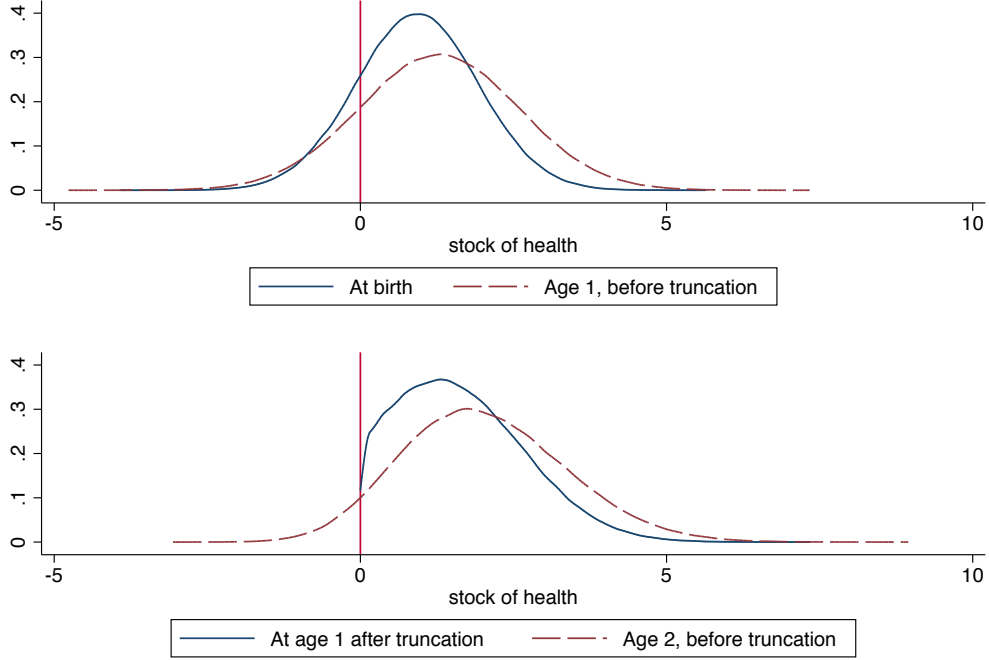
Appendix A1: Figures

Figure 6: Comparison of q-rate in the paper and HMD (1816)
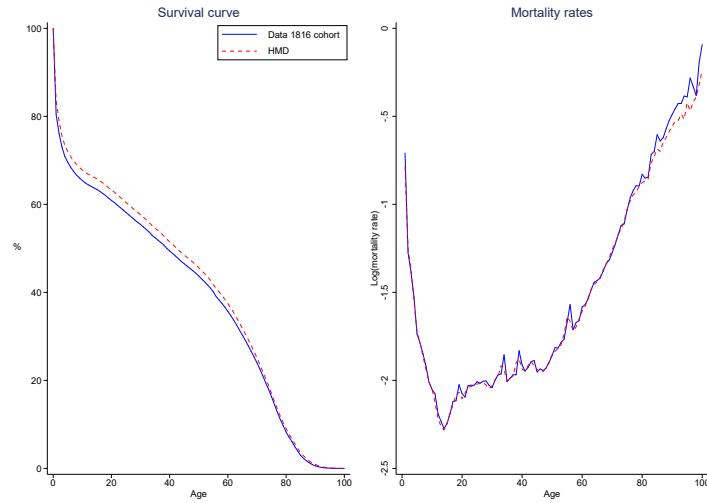
Note: The life expectancy is 38.25 years with the q we use, to be compared with 39.86 with the q in HMD and 39.83 years for the life expectancy computed by the HMD itself following a more involved statistical methodology.

Figure 7: Health and mortality in the first two years of life

Data from simulations

In the first period the (infant) mortality rate MR_1 is given by

$$MR_1 = P(H_1 \leq \underline{H}) = P\left(H_0 + I - \delta + \varepsilon_1 \leq \underline{H}\right)$$

$$= P(\varepsilon_1 \leq \varphi_1) = F(\varphi_1)$$

where $\varphi_1 = \underline{H} - I + \delta - H_0$ captures the threshold for dying in period 1 in terms of the random shock. Investments lower this threshold (lower mortality) and depreciation increases it (increases mortality).

Consider now the probability of dying at age $t = 2$. This is given by the probability that the stock falls below $\underline{H}$ at age 2, conditional on having survived to age 2, which can be expressed as:

$$
\begin{aligned}
MR_2 &= E(D_2 = 1 | D_1 = 0) = P(H_2 < \underline{H} | H_1 > \underline{H}) \\
&= \frac{P(H_2 < \underline{H}, H_1 > \underline{H})}{P(H_1 > \underline{H} | g_1, g_2)} = \frac{P(\varepsilon_2 < \varphi_2 - \varepsilon_1, \varepsilon_1 > \varphi_1)}{1 - F(\varphi_1)} \\
&= \frac{K(\varphi_2, \varphi_1)}{1 - F(\varphi_1)}
\end{aligned}
\tag{1}
$$

where $\varphi_2 = \underline{H} - I + \delta 2^\alpha - H_0$ captures the threshold for dying in period 2, and $K(\varphi_2, \varphi_1) = \int_{\varepsilon_1 = \varphi_1}^{\infty} \int_{\varepsilon_2 = -\infty}^{\varphi_2 - \varepsilon_1} f(\varepsilon_1) f(\varepsilon_2) d\varepsilon_1 d\varepsilon_2$ is the density right above the old threshold and below the new threshold, that is the fraction of survivors who dies as a result of a new shock. The denominator is the fraction of survivors.

Figure 8: Model behavior

(a) The evolution of the health distribution over the lifetime
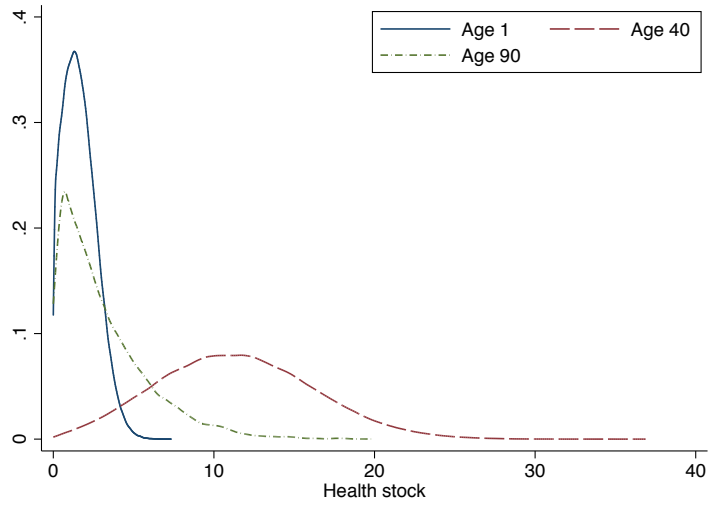
(b) Age profile of population health and mortality
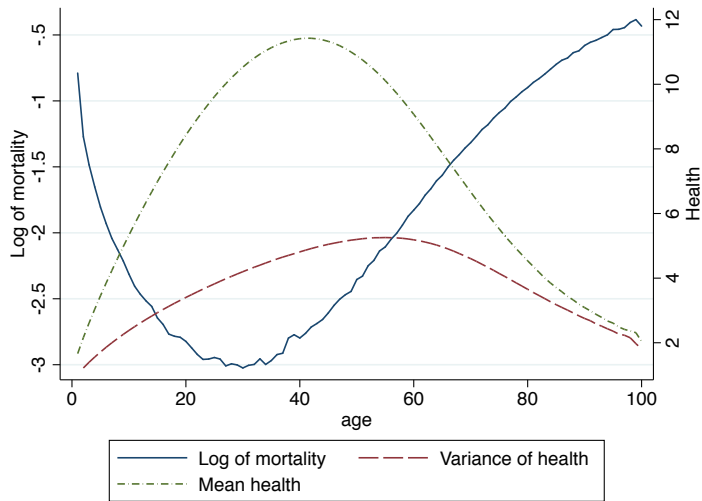
Note: Simulated data for a population of 500,000 individuals. For this simulation we use the following parameters: I=0.3575753, δ=0.0004789, σ=0.8353752, α=1.7883, μ_0=0.925079. *Panel a* shows the density of health for the population at ages 1, 40 and 90. *Panel b* plots the average health, the variance of health and the mortality rates of the population over the lifetime.

Figure 9: Adding accidents to the baseline model
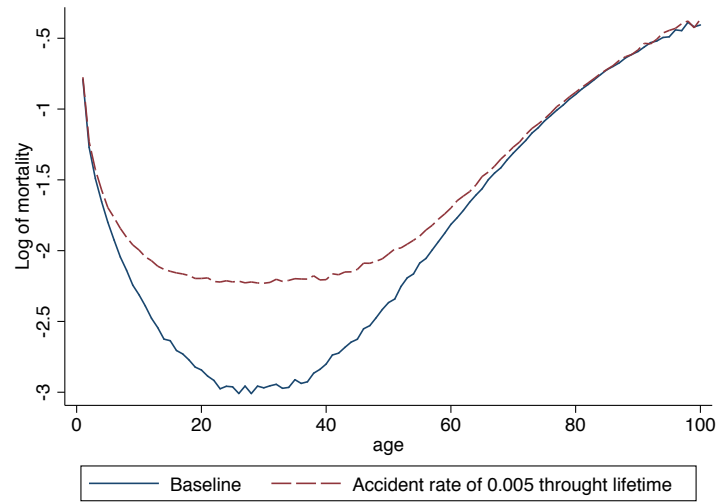
Note: The baseline parameters are the same as in Figure 8b. The red dashed line shows the mortality curve of a population that experiences a 0.005 percent chance of dying every period due to an accident, unrelated to health. Mortality rates are higher at all ages but more so in middle ages in proportional terms, because of competing risks. Many younger and older individuals that are hit by an accident shock are also unhealthy and would die even in the absence of an accident shock.

Figure 10: US Age-specific Mortality rates per 1,000 in 1990, by age and cause of death
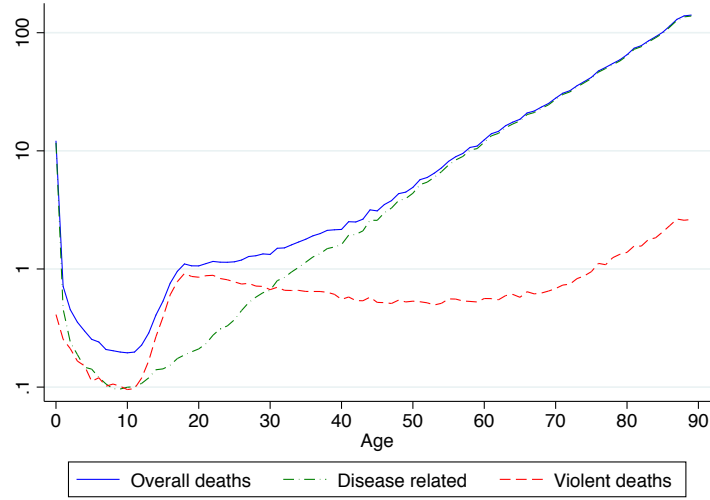
Note: this figure is reproduced from Schwandt and von Wachter (2018)'s paper "Mortality Profiles of Unlucky Cohorts: Effects of Entering the Labor Market in a Recession on Longevity" who generously agreed to let us use it. The data come from period (not cohort tables) so they are not directly comparable to ours but we use it to demonstrate that the mortality rate from non-disease related causes of death is well approximated by a step function turns on in adolescence. Mortality rates are shown in log(10) scale.

Figure 11: Cohort vs. Period Mortality Rates, French Women 1860 and 1940
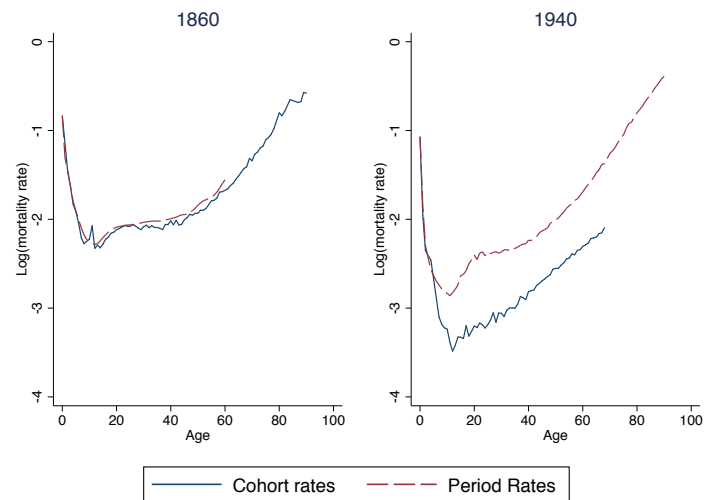
Note: Data from the Human Mortality Database. Period and cohort mortality rates were almost identical for the cohort born in 1860, suggesting that for these cohorts the assumption of stationarity holds. In other words, the mortality rate at age 50 of a French woman born in 1860 is about the same as the one of a French woman who is 50 year old in 1860. In 1940 a large gap has appeared and the cohort mortality rates is significantly lower than the period rate.

Figure 12: Age profile of mortality of women born in France between 1860 and 1940, by decade

Log-Mortality Rates. French Women cohorts born between 1860 and 1939 (Source:HMD)
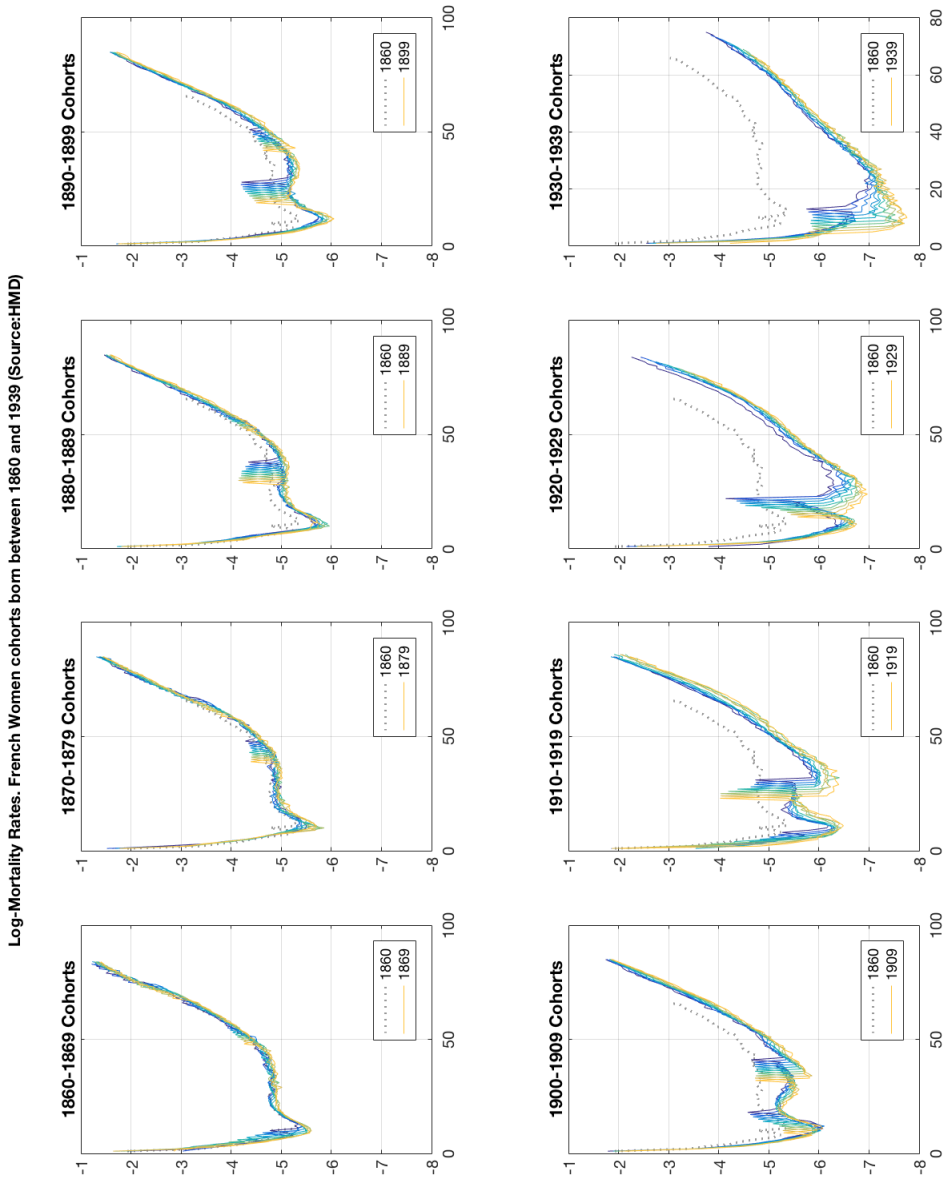
Note: Human Mortality Data

Figure 13: Estimated Aging Function for the 1816 and 1916 cohorts
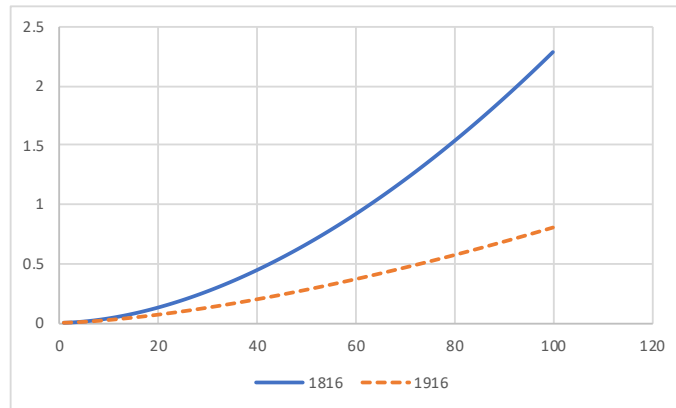
Note: This figure shows the estimated aging function $\delta * t^{\alpha}$ for the 1816 cohort ($0.0006 \cdot t^{1.79}$) and the 1916 ($0.0007 \cdot t^{1.53}$) cohort. It shows that the aging rate has flattened dramatically due to a 15% decline in α.

Figure 14: Effects of decreasing annual health investments I throughout the lifetime by 50%
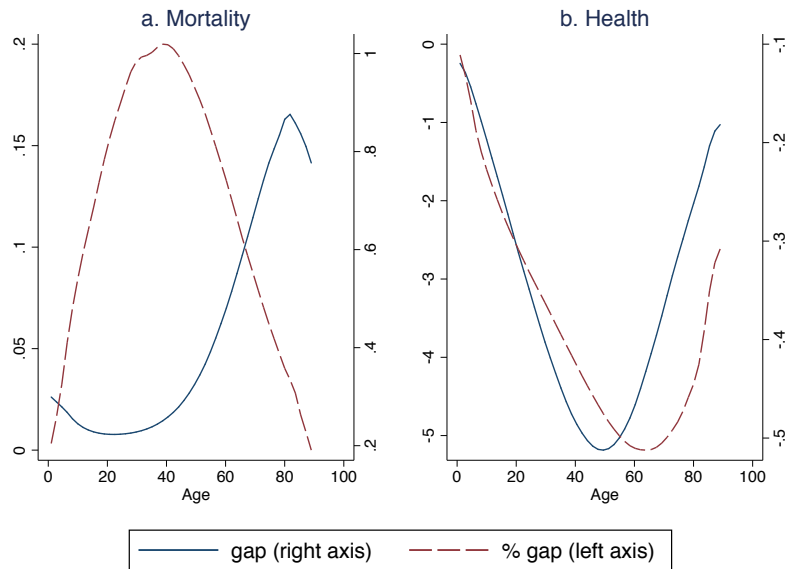
Note: The Figure shows the simulated effects of increasing the baseline level of I by 50%. We plot the gap between the baseline and the affected population. This gap is computed as MR(low)-MR(high), or H(low)-H(high). *Panel a* shows the effects on mortality in both levels and percentage terms, and *panel b* shows the effects on health. The baseline parameters are the same as in Figure 8b.

Figure 15: Increasing the lifetime depreciation rate by 50% by age
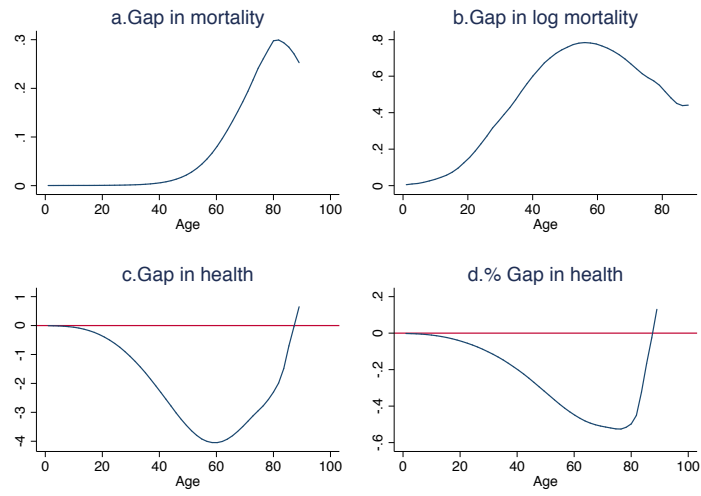
Note: The Figure shows the gap in mortality or health between a baseline population and a population with a 50% higher depreciation rate δ. Gap is computed as MR(low)-MR(high), or H(low)-H(high). The figures become very noisy after age 90 because there are almost no survivors, so we do not include these data points. Simulated data for two population of 500,000 individuals each. The baseline parameters are the same as in Figure 8b.

Figure 16: Effects of in-utero shocks on health and mortality

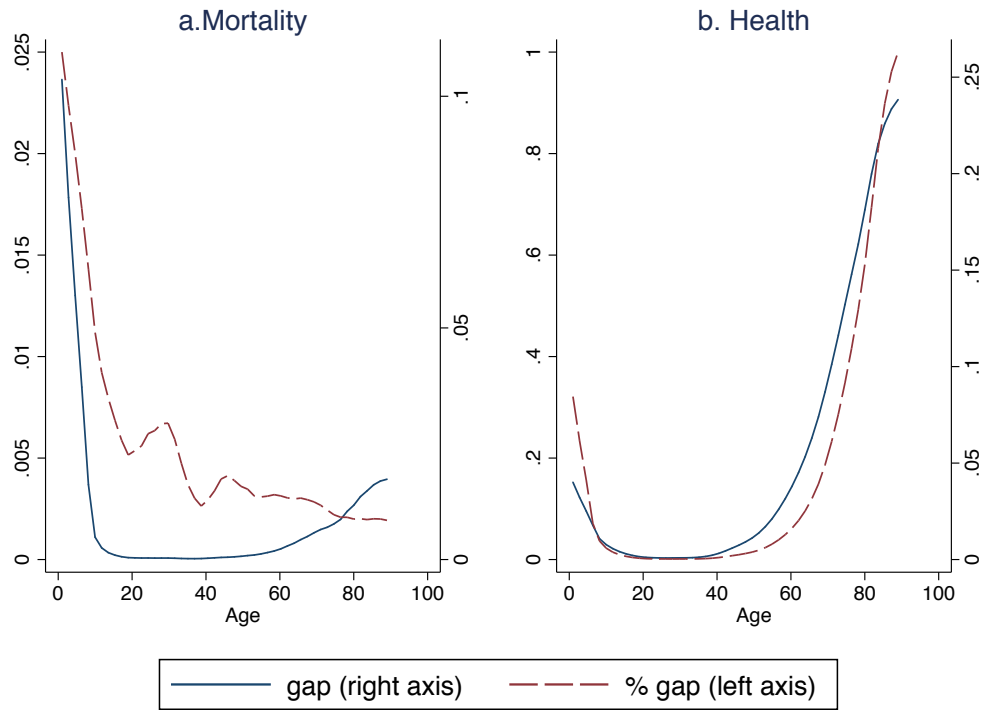Note: The Figure shows the simulated effects of decreasing the baseline level of μ by 50%. We plot the gap between the baseline and the affected population. This gap is computed as MR(low)-MR(high), or H(low)-H(high). *Panel a* shows the effects on mortality in both levels and percentage terms, and *panel b* shows the effects on health. The baseline parameters are the same as in Figure 8b.

Figure 17: Effect of exogenous temporary shocks at age 20 on log mortality
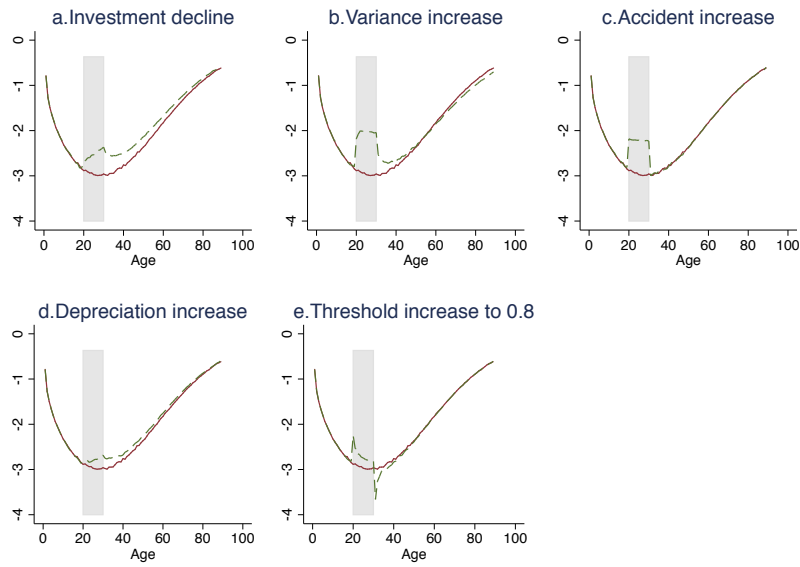
Note: The Figure shows the effects of a temporary change in a single parameter occuring at age 20. The shaded area corresponds to the years of the temporary shock. Each type of shock leaevs a unique imprint on the mortality curves. One temporary changes in the threshold generate mortality that is abnormally low right after the shock ends. The baseline parameters are the same as in Figure 8b.

Appendix A2: Tables

Table 1: Modeling prime-age mortality. French Women born in 1816

		(0)	(4)
Model for hump: change in...		Baseline	With adolescent hump
Initial mean health	μ_H	0.9115	0.8634
Investment	I	0.1336	0.4075
Standard Deviation of Shock	σ_e	0.5556	1.0241
Depreciation	δ	0.0010	0.0006
Aging	α	1.4350	1.7849
Adolescent Hump*	κ		0.0086
Fit (survival curve)^		155.06	12.36
Fit (log of q_x)		3.01	0.74
Fit (death distribution)**		6.21	3.35
Actual Life Expectancy	38.25		
Predicted Life Expectancy		38.43	38.28
Counterfactual Life expectancy^^			45.86

In this table we fit the model to the 1816 population with and without an exogenous increase in the accident rate occurring in adolescence.

*The estimate in this row corresponds to the value of the parameter κ after the onset of adolescence. Adolescence starts at age = (- 0.0175 x calendar year) + 47.4 for all women, based on the estimates provided in de La Rochebrochard (2000).

**To make the fit of the age distribution comparable across columns we use the (normalized) number of deaths as weights.

^Our main fit criteria is the sum of squared errors of the survival rate at each age We also report the fit as the sum of squared errors of the log of q_x (the probability of dying between ages x and $x + 1$) and the distribution of deaths. We don't target these moments directly–we target the survival curve.

^^Counterfactual Life Expectancy is computed by holding all estimated parameters fixed and setting the adolescent hump to 0.

Table 2: Estimated parameters for female chimpanzees living in the wild

Gender		Basic model	With adolescent hump
Initial mean health	μ_H	0.9783	1.0043
Investment (annual)	I	0.3295	0.3390
Standard Deviation of Shock	σ_e	1.0871	1.1304
Depreciation	δ	0.0560	0.0553
Aging	α	0.7677	0.7820
Adolescent Hump*	κ		0.00001
# of individuals at birth		80	80
# of moments reported		55	55
Fit (survival curve)[b]		112.50	111.29
Fit (log of q_x)		2.11	2.11
Actual Life Expectancy		$15.38(13.4)^a$	
Predicted Life Expectancy		15.35	15.35

The first column estimates the model without an adolescent hump. The second model estimates the model with an exogenous increase in accidents in adolescence. Because the data are noisy the second model is not a substantially better fit than the first. Both are however excellent fits for this population.

Data sources: Life tables for primates in the wild come from Bronikowski et al. (2011). In the wild population data come from Brazil, Costa Rica, Kenya, Tanzania, Madagascar and Rwanda.

a. Life expectancy in parenthesis corresponds to the one reported in Bronikowski et al. (2011).

b. We target the survival curve and compute the sum of squared errors – the data provided are in the form of survival rates.

*Adolescence starts at age 8.

Table 3: Robustness checks for 1816

		(1)	(2)	(3)	(4)	(5)	(6)	(7)
		Basic	κ_b	κ_b at $T{\sim}N()$	$T{\sim}N()$ estimated	Weight	Target death	Truncation at 90
Initial mean health	μ_H	0.8634	0.8917	0.8635	0.7503	0.8020	0.7327	0.8784
Investment	I	0.4075	0.4322	0.4149	0.3712	0.4180	0.4743	0.4200
Standard Deviation of Shock	σ_e	1.0241	1.0713	1.0367	0.8369	0.9971	0.9930	1.0552
Depreciation	δ	0.0006	0.0005	0.0005	0.0005	0.0006	0.0006	0.0006
Aging	α	1.7849	1.8321	1.8153	1.8011	1.7807	1.7950	1.7973
Adolescent Hump*	κ_a	0.0086	0.0089	0.0089	0.0112	0.0093	0.0108	0.0087
Accident rate before adolescence	κ_b		0.0005					
Mean*				15.6	14.29			
Standard deviation*				1.32	15.71			
Fit (survival curve)^		12.36	13.03	11.49	3.75	15.86	173.74	12.36
Fit (log of q_x)		0.74	0.65	0.57	0.40	0.92	1.93	0.56
Fit (death distribution)**		3.35	39.55	21.82	2.25	6.89	4.48	28.17
Actual Life Expectancy					38.25			
Predicted Life Expectancy		38.28	38.29	38.28	38.26	38.33	39.27	38.27
Counterfactual Life expectancy^^		45.86	46.45	46.08	48.82	46.66	49.49	45.86

*Adolescence starts at age = (- 0.0175 x calendar year) + 47.4 in columns 1, 2, 5, 6 and 7. In column 3 the timing of adolescence is assumed to follow a normal distribution with mean value (- 0.0175 x calendar year) + 47.4, and standard deviation 1.3285, calculated from the table of 1975 girls in de La Rochebrochard (2000).

In column 4 we estimate the mean and the standard deviation of the onset of adolescence.

In column 5 we investigate what happens if we use the (normalized) number of deaths as weights in the estimation. In column 6 we use weights and target the distribution of the ages at death instead of the survival curve. In the column 7 we use only data up to age 90 to see what the effect of censoring is and because the data after 90 are estimated. The estimates are somewhat sensitive to these choices. The predicted life expectancy is very close in all cases (the error in the predicted life expectancy is less then 0.1 years of life), except when we target the age at death distribution (the prediction is off by about a year). But the counterfactual predictions are sensitive: eliminating the hump results in a loss of life of 7.58 years on the baseline model and 9.81 in the worse model.

^Our main fit criteria is the sum of squared errors of the survival rate at each age. We also report the fit as the sum of squared errors of the log of q_x (the probability of dying between ages x and $x+1$) and the distribution of deaths. We don't target these moments directly–we target the survival curve.

^^Counterfactual Life Expectancy is computed by holding all estimated parameters fixed and setting the adolescent hump to 0.

**To make the fit of the age distribution comparable across columns we use the (normalized) number of deaths as weights.

In column 4 we target the survival curve but use the (normalized) number of deaths as weights

In column 5 we target the distribution of the age at death and we use the number of deaths as weights.

Table 4: Estimated parameters for WWII for French Women born in 1921

		(1)	(2)	(3)	(4)	(5)
Model for WWII: change in...		I	κ	σ_e	$\underline{H}$	δ
Initial condition	μ_H	0.9790	1.0837	1.0638	1.0522	1.0875
Investment	I	0.2985	0.2739	0.2650	0.2385	0.2597
Standard Deviation of Shock	σ_e	0.4255	0.4561	0.4358	0.3891	0.4412
Depreciation	δ	0.0007	0.0008	0.0009	0.0008	0.0008
Aging	α	1.5358	1.5272	1.4961	1.4785	1.5121
Adolescence Hump*	κ	0.0026	0.0030	0.0032	0.0031	0.0032
WWII Shock**		-0.1173	0.0036	0.3495	0.8919	0.0000
Fit (survival curve)^		40.62	37.02	38.49	38.53	38.88
Fit (log of q_x)		4.87	2.69	3.11	3.29	2.87
Fit during WWII (log of q_x)		0.21	0.53	0.68	0.73	0.68
% Difference in # deaths during WWII~~		-0.21	-0.36	-0.45	-0.32	-0.45
Actual Life Expectancy				66.00		
Predicted Life Expectancy		66.03	66.03	66.02	66.03	66.02
Counterfactual Life expectancy^^		70.90	66.24	65.94	66.23	65.05
Actual Life expectancy in 1946				55.93		
Life expectancy in 1946		55.27	55.25	55.12	55.28	55.16
Counterfactual LE in 1946		60.36	55.24	55.05	55.17	54.00

*Hump is modeled as a accident rate that starts in adolescence, set to happen at (- 0.0175 * calendar year) + 47.4 based on the estimates provided in de La Rochebrochard (2000).

**The estimates in this row corresponds to the value of the parameter during the war. For example the first column shows that I was about 0.299 throughout life but decreased to -0.117 during the war. The same applies to columns (3) and (4), the standard deviation decreases from 0.436 to 0.350 and the threshold moves from 0 to 0.892. In column 2, we estimate the value of an additional random shock during the war, an approximate 41% decrease relative to the adolescent hump (but since the shock is independent this is only approximate).

^Our main fit criteria is the sum of squared errors of the survival rate at each age We also report the fit as the sum of squared errors of the log of q_x (the probability of dying between ages x and $x + 1$). We don't target these moments directly–we target the survival curve.

^^Counterfactual Life Expectancy is computed by holding all estimated parameters fixed and setting the war parameters to 0.

~This is computed as sum of squared errors during the war years. A lower number is better.

~~This is computed as (predicted - actual)/actual

To make the fit of the age distribution comparable across columns we use the (normalized) number of deaths as weights.

Appendix B: Mathematical Details and Proofs omitted in the text

Before proving the propositions contained in the text we examine the identification of the model. The model is defined as follows:

$$\begin{cases} H_t = H_{t-1} - d(t) + I + \varepsilon_t & \text{if } D_{t-1} = 0 \\ D_t = \mathbb{I}(H_t \leq \underline{H}, D_{t-1} = 0), \\ D_0 = 0 \end{cases} \tag{2}$$

with $d(t) = \delta \cdot t^\alpha$ $\delta \in (0, \infty), \alpha \in (0, \infty),$ and $I \in \mathbb{R}$. $\underline{H}$ and σ_H^2 are normalized to be 0 and 1, respectively. Let $\hat{H}_t \equiv \mathbb{E}[H_t \mid H_t > 0]$ denote the average health in the living population with age t and $\sigma_{\hat{H}_t} \equiv Var[H_t \mid H_t > 0]$ the variance of health among the living.

Identification. Suppose that we have two sets of parameters $\theta = (I, \delta, \sigma_\varepsilon, \alpha, \mu_H)$ and $\theta' = (I', \delta', \sigma'_\varepsilon, \alpha', \mu'_H)$. We say that θ and θ' are *observationally equivalent* (OE) if they generate the same mortality rates at each age, that is, if nd only if

$$MR_t(\theta) = MR_t(\theta'), \forall t \in \mathbb{N}$$

Equivalently, we could define observational equivalence in terms of survival rates $\{S_t(\theta)\}_{t>0}$ since each sequence can be uniquely recovered from the other one. Because the model does not have a closed-form solution for the mortality rates, proving the identification formally takes several steps. A key step is to use an "identification at infinity" argument to prove that the variances σ_ε and σ'_ε must be the same. Then identification of the remaining parameters follows.

We first distinguish two theoretical cases. We say that θ and θ' are *weakly observationally equivalent* (W.O.E.) if and only if 1) θ and θ' are O.E. and 2) they do not generate the same sequences of health distributions, i.e.

$$\begin{cases} \exists t \in \mathbb{N}, \exists x \in \mathbb{R}^+ & F_{H_t}(x; \theta) \neq F_{H_t}(x; \theta') \\ \forall t \in \mathbb{N} & MR_t(\theta) = MR_t(\theta') \end{cases}$$

In contrast, we say that θ and θ' are *strongly observationally equivalent* (S.O.E.) iff 1) θ and θ' are O.E. and 2) they generate the same sequences of health distributions, i.e.

$$\begin{cases} \forall t \in \mathbb{N}, & F_{H_t}(\cdot; \theta) = F_{H_t}(\cdot; \theta') \\ \forall t \in \mathbb{N} & MR_t(\theta) = MR_t(\theta') \end{cases}$$

Although we cannot distinguish between O.E. and W.O.E. by observing mortality rate only, we could in principle observe some other features of the distributions of health at all ages that could break the identification.[28] Towards a contradiction, suppose that θ and θ' are O.E., with $\theta' \neq \theta$. Then two cases must be considered, whether they are weakly or strongly observationally equivalent. We first show that strong observational equivalence is not possible.

Suppose that $(I, \delta, \alpha, \mu_H) \neq (I', \delta', \alpha', \mu'_H)$, then these two sets of parameters cannot generate the same first four modes of the health distribution and therefore are not observationally equivalent. The first four modes are

---

[28] A step in that direction would be to observe a good proxy for health for a cohort.

$$mode(1) = \mu_H + I - \delta$$
$$mode(2) = \mu_H + 2I - \delta(1 + 2^\alpha)$$
$$mode(3) = \mu_H + 3I - \delta(1 + 2^\alpha + 3^\alpha) \tag{3}$$
$$mode(4) = \mu_H + 4I - \delta(1 + 2^\alpha + 3^\alpha + 4^\alpha)$$

These equations can be manipulated to obtain a triangular system: the difference between consecutive modes eliminate μ_H, $m_4 - m_3 = I - \delta 4^\alpha$, a double difference $(m_4 - m_3) - (m_3 - m_2)$ further eliminates I and finally dividing this double difference by another one, $m_3 - m_2 - m_2 - m_1$ eliminates δ. Now suppose that $(I, \delta, \alpha, \mu_H) = (I', \delta', \alpha', \mu_H')$ and $\sigma_\varepsilon \neq \sigma_\varepsilon'$ then the first two mortality rates cannot be equal

$$m_1(\theta) = \Phi\left(\frac{-\mu_H - I + \delta}{\sqrt{1 + \sigma_\varepsilon^2}}\right) \neq \Phi\left(\frac{-\mu_H - I + \delta}{\sqrt{1 + (\sigma_\varepsilon')^2}}\right) = m_1(\theta') \tag{4}$$

We now consider weak observational equivalence, i.e. the case where different sets of parameters produce different health distributions nonetheless delivering the same mortality rates. Let us define the first time at which the two health distribution differ $\tau \equiv \min\{t \in \mathbb{N} \mid \exists x \in \mathbb{R}^+ \ F_{H_t}(x; \theta) \neq F_{H_t}(x; \theta')\}$. It is well defined by definition of weakly observational equivalence. Because F_{H_t} is continuous except at 0, we can assume without loss of generosity that the two cdf differ on some non trivial interval $(a, b) \supset \{x\}$. If $\tau > 1$ then because at the previous period the two distribution are the same, it must be the case that $\sigma_\varepsilon \neq \sigma_\varepsilon'$, otherwise the tails could not be similar. So it must be that $\tau = 1$ i.e. the distribution start differing at the first period.

Lemma 1. *The variance is separately identified.*

If the probability of surviving until age t , $\{S_t\}_{t \in [0,T]}$, is observed for an arbitrary large T. Then the variance is identified. Intuitively, the variance of the shock characterizes the thickness of the right-hand tail. If one population has a larger variance than the other one then the ratio of survivors grows arbitrarily large at old age. More formally, let $\theta = \{\sigma, \psi\}$ denote the set of parameters. For any ψ, ψ' such that

$$\sigma > \sigma' \implies \lim_{t \to +\infty} \frac{S_t(\sigma, \psi)}{S_t(\sigma', \psi')} = +\infty \tag{5}$$

Let $\psi = \{\alpha, \delta, \mu_0, \kappa\}$ and $\sigma > \sigma'$. We have that for any t $\lim_{t \to +\infty} \frac{f_{H_t}(x; \sigma, \psi)}{f_{H_t}(x; \sigma', \psi')} = +\infty$. The only way to "compensate" for a small variance, which creates in old ages a right tail of very healthy people is to have a lower depreciation (δ and α). However because the tail decreases at exponential rate, we have

$$\lim_{t \to +\infty} \frac{f_{H_t}(x + z_t; \sigma, \psi)}{f_{H_t}(x; \sigma', \psi')} = +\infty \ \forall x > 0 \tag{6}$$

where $z_t = \sum_{s<t} \delta t^\alpha - \sum_{s<t} \delta' t^{\alpha'}$. This is an "identification at infinity" argument (see Chamberlain (1986), Heckman (1990)). For estimation purpose, however, this method is sensitive to the quality of the data sample. In our case, we verified by simulation that close values of σ can be difficult to distinguish as sampling error because larger for very old ages.

Lemma 2. *For any t, one of these cases occurs: either (1) f_{H_t} is hump-shaped (increasing then decreasing) or (2) f_{H_t} is strictly decreasing.*

The initial distribution and the shocks at every age are normal distributions, which are log-concave. The probability density function of a sum of two random variables is the convolution of their probability density functions. The space of log concave is closed under convolution (Ibragimov (1956)) and Log-concavity implies single-peakedness. Log-concavity is not affected by the truncation either, until the point where the mode of the distribution at time t lies in the interval $(0, \delta (t+1)^\alpha - I)$. During the following period, the mode after convolution falls below 0 and the distribution becomes strictly decreasing henceforth.

Corollary 1. *There exists $t_{mode} > 0$ such that*

$$
\begin{cases}
mode\,(f_{H_t}) > 0 & t < t_{mode} \\
mode\,(f_{H_t}) = 0 & t \geq t_{mode}
\end{cases}
$$

where the mode of the distribution is

$$
\max \left\{ \mu_0 + I \cdot t - \delta \sum_{s=0}^{t} s^\alpha, 0^+ \right\}
$$

Proposition 1. *Everyone dies eventually.*

The cumulative distribution function of our process can be bounded above by a process easier to study. Consider the process $\{H_t^*\}_{t=1}^{\infty}$, defined by $H_0^* = H_0 \sim \mathcal{N}\left(\mu_H, \sigma_H^2\right)$ and the recurrence relation:

$$
H_t^* = H_{t-1}^* + I - \delta \cdot t^\alpha + \varepsilon_t \,, \ \varepsilon_t \sim \mathcal{N}\left(0, \sigma_\varepsilon^2\right) \tag{7}
$$

The process is similar to the one in our model except that there is no truncation. It is easy to tell that $0 \leq P\left(H_t > z\right) \leq P\left(H_t^* > z\right)$ for any $z > 0$. Now for any $t \geq 0$, H_t^* is normally distributed with mean

$$
\mu_{H_t^*} = \mu_H + I \cdot t - \delta \sum_{k=1}^{t} k^\alpha \tag{8}
$$

and standard deviation

$$
\sigma_{H_t^*} = \sqrt{\sigma_H^2 + t \cdot \sigma_\varepsilon^2} \tag{9}
$$

Hence, $P\left(H_t^* > z\right) = 1 - \Phi(\frac{z - \mu_{H_t^*}}{\sigma_{H_t^*}})$, where Φ is the CDF of the standard normal distribution. As $t \to \infty$, we have $\mu_{H_t^*} \sim I \cdot t - \delta \cdot \frac{t^{\alpha+1}}{\alpha+1}$ and $\sigma_{H_t^*} \sim \sqrt{t} \cdot \sigma_\varepsilon$. Therefore if $\alpha > 0$, $\frac{\mu_{H_t^*}}{\sigma_{H_t^*}} \to -\infty$ as $t \to \infty$.

Proposition 2. *Increasing the investment I reduces the mortality rates at all ages.*

Let $a_t = I - \delta t^\alpha$. The random variable H_t has a mass point at $z = 0$ but is continuous on $(0, +\infty)$. $F_{H_t}(0)$ is the probability of not surviving until age t while for any $z > 0$, the cdf can be expressed

$$
F_{H_t}(z) = \int_{x=0}^{\infty} \Phi\left(\frac{z - a_t - x}{\sigma_\varepsilon}\right) f_{H_{t-1}}(x)\,dx + F_{H_{t-1}}(0) \tag{10}
$$

Equivalently, after integration by parts, one obtains:

$$
F_{H_t}(z) = -\frac{1}{\sigma_\varepsilon} \int_{x=0}^{\infty} \phi\left(\frac{z - a_t - x}{\sigma_\varepsilon}\right) F_{H_{t-1}}(x)\,dx + F_{H_{t-1}}(0) \tag{11}
$$

Hence the mortality rate at age t, which is the probability of dying at age t conditional on surviving until age t, can be written:

$$MR_t = \frac{F_{H_t}(0) - F_{H_{t-1}}(0)}{1 - F_{H_{t-1}}(0)}$$

Suppose that for every t we increase the constant investment level I to some level $I' > I$. Following the expression above, the impact can be be decomposed in two: first, a direct effect on the probability of dying at age t (the numerator) and, second, a compounded effect carried through the distribution of health for those attaining age t.We show that, for any t, both effects go in the same direction: an increase in I simultaneously increases the probability of surviving until age t (hence increases the denominator) and reduces the probability of dying at age t (the numerator goes down). We prove the following lemma.

Lemma 3. *For all t, we have:*
1. $\forall z \geqslant 0$, $\frac{\partial F_{H_t}(z; I)}{\partial I} \leq 0$
2. $\frac{\partial MR_t}{\partial I} \leq 0$

Proof: We prove these inequalities jointly and by induction. Notice that $\frac{\partial F_{H_t}(\cdot; I)}{\partial I} \leq 0$ signifies that the cdf's are ranked by first order stochastic dominance. The higher the I, the further the distribution is pushed to the right, which decreases the value of the cdf at any point x as I increases. Because all the individuals would then be in better health, ceteris paribus, fewer of them will die each period. Combined with a higher denominator, this delivers a lower mortality rate at each point.

At $t = 0$: $F_{H_1}(z; I) = \Phi\left(\frac{z - \mu_0}{\sigma_0}\right)$ hence $\frac{\partial F_{H_1}(z; I)}{\partial I} = 0$. $MR_t = F_{H_t}(0) = \Phi\left(\frac{z - \mu_0}{\sigma_0}\right)$ which, again, is non-increasing with I. In period 1, we have $\forall z \geqslant 0$,

$$
\begin{aligned}
F_{H_1}(z) &= Pr(H_0 + I - \delta + \varepsilon_1 \leqslant z) \\
&= Pr(H_0 + \varepsilon_1 \leqslant z + \delta - I) \\
&= \Phi\left(\frac{z + \delta - I - \mu_H}{\sqrt{1 + \sigma_\varepsilon^2}}\right)
\end{aligned}
\tag{12}
$$

therefore in terms of mortality rates we have

$$
\begin{aligned}
MR_1 &= Pr(H_1 \leqslant 0) \\
&= Pr(H_0 + I - \delta + \varepsilon_1 \leqslant 0) \\
&= \Phi\left(\frac{\delta - I - \mu_H}{\sqrt{1 + \sigma_\varepsilon^2}}\right)
\end{aligned}
\tag{13}
$$

It is easy to see that as I or μ_H increases, both $F_{H_1}(z)$ and MR_1 decreases. We have, $\forall t \geqslant 2, \forall z \geqslant 0$,

$$
\begin{aligned}
F_{H_t}(z) &= Pr(H_t \leqslant z) \\
&= Pr(H_t \leqslant z, H_{t-1} > 0) + Pr(H_t \leqslant z, H_{t-1} \leqslant 0) \\
&= Pr(H_{t-1} + I - \delta t^\alpha + \varepsilon_t \leqslant z, H_{t-1} > 0) + Pr(H_{t-1} \leqslant 0) \\
&= Pr(0 < H_{t-1} \leqslant z + \delta t^\alpha - I - \varepsilon_t) + Pr(H_{t-1} \leqslant 0) \\
&= \frac{1}{\sigma_\varepsilon} \int_{x=0}^{\infty} \phi\left(\frac{x - z - \delta t^\alpha + I}{\sigma_\varepsilon}\right) \left(F_{H_{t-1}}(x) - F_{H_{t-1}}(0)\right) dx + F_{H_{t-1}}(0)
\end{aligned}
\tag{14}
$$

$$MR_t = \frac{F_{H_t}(0) - F_{H_{t-1}}(0)}{1 - F_{H_{t-1}}(0)} \tag{15}$$

Then

$$
\begin{aligned}
\frac{\partial F_{H_t}(z; I)}{\partial I} \\
=& \frac{\partial}{\partial I} \left(\frac{1}{\sigma_\varepsilon} \int_{x=0}^\infty \phi\left(\frac{x - z - \delta t^\alpha + I}{\sigma_\varepsilon} \right) \left(F_{H_{t-1}}(x) - F_{H_{t-1}}(0) \right) dx \right) + \frac{\partial F_{H_{t-1}}(0; I)}{\partial I} \\
=& \frac{1}{\sigma_\varepsilon^2} \int_{x=0}^\infty \phi'\left(\frac{x - z - \delta t^\alpha + I}{\sigma_\varepsilon} \right) \left(F_{H_{t-1}}(x) - F_{H_{t-1}}(0) \right) dx \\
& + \frac{1}{\sigma_\varepsilon} \int_{x=0}^\infty \phi\left(\frac{x - z - \delta t^\alpha + I}{\sigma_\varepsilon} \right) \left(\frac{\partial F_{H_{t-1}}(x; I)}{\partial I} - \frac{\partial F_{H_{t-1}}(0; I)}{\partial I} \right) dx \\
& + \frac{\partial F_{H_{t-1}}(0; I)}{\partial I} \\
=& \frac{1}{\sigma_\varepsilon^2} \int_{x=0}^\infty \phi'\left(\frac{x - z - \delta t^\alpha + I}{\sigma_\varepsilon} \right) \left(F_{H_{t-1}}(x) - F_{H_{t-1}}(0) \right) dx \\
& + \frac{1}{\sigma_\varepsilon} \int_{x=0}^\infty \phi\left(\frac{x - z - \delta t^\alpha + I}{\sigma_\varepsilon} \right) \frac{\partial F_{H_{t-1}}(x; I)}{\partial I} dx \\
& + \Phi\left(-z - \delta t^\alpha + I \right) \frac{\partial F_{H_{t-1}}(0; I)}{\partial I}
\end{aligned}
\tag{16}
$$

All three items are negative, so we have

$$
\frac{\partial F_{H_t}(z; I)}{\partial I} \leqslant 0
\tag{17}
$$

Differentiating the mortality rates with respect to investments, we have

$$
\begin{aligned}
& \frac{\partial MR_t}{\partial I} \\
=& \frac{1}{(1 - F_{t-1}(0))^2} \left(\frac{\partial F_{H_t}(0)}{\partial I}(1 - F_{H_{t-1}}(0)) - \frac{\partial F_{H_{t-1}}(0)}{\partial I}(1 - F_{H_t}(0)) \right) \\
\leq& 0
\end{aligned}
\tag{18}
$$

Remark: Increasing any of the aging parameters, δ or α increases the mortality rate at all ages.

The exact same proof applies for δ and α as their impact on F_{H_t} through the aging function a_t, is similar to the effect of I.

Proposition 3. *Investment and health at birth are complements*

The proof builds on the proof of the effect of I on the mortality rates. In addition, we have that

$$
\begin{aligned}
\frac{\partial^2 F_{H_{t_2}}(z; \mathcal{I})}{\partial I_{t_1} \partial I_{t_2}} &= \frac{\partial}{\partial I_{t_1}} \frac{\partial}{\partial I_{t_2}} \left[-\frac{1}{\sigma_\varepsilon} \int_{x=0}^\infty \phi\left(\frac{z - x - I_{t_2} + \delta(t_2)^\alpha}{\sigma_\varepsilon} \right) \left(F_{H_{t_2-1}}\left(x, \mathcal{I} - F_{H_{t_2-1}}(0) \right) \right) dx \right] \\
& \quad + \frac{\partial}{\partial I_{t_1}} \frac{\partial F_{H_{t_2-1}}(0; \mathcal{I})}{\partial I_2} \\
&= \frac{\partial}{\partial I_{t_1}} \left[\frac{1}{\sigma_\varepsilon^2} \int_{x=0}^\infty \phi'\left(\frac{z - x - a_t}{\sigma_\varepsilon} \right) \left(F_{H_{t_2-1}}(x, \mathcal{I}) - F_{H_{t_2-1}}(0) \right) dx \right] + 0 \\
&= \frac{1}{\sigma_\varepsilon^2} \int_{x=0}^\infty \phi'\left(\frac{z - x - a_t}{\sigma_\varepsilon} \right) \left(\frac{\partial}{\partial I_{t_1}} F_{H_{t_2-1}}(x, \mathcal{I}) - \frac{\partial}{\partial I_{t_1}} F_{H_{t_2-1}}(0) \right) dx \\
&\leq 0
\end{aligned}
\tag{19}
$$

because $\frac{\partial}{\partial I_{t_1}} F_{H_{t_2-1}}(x, \mathcal{I}) \leq 0$ (increasing investment at time 1 creates a FOSD distribution). And as a consequence the denominator $1 - F_{H_{t_2-1}}(0)$ goes up as well.

Remark: Extended model with Accident shocks Proposition 1, 2 and 3 hold for the extended model with accident shocks drawn indepently from the health status. This is because of independence, the accident shock leaves the health *C.D.F.* unchanged and therefore the proofs are unaffected.

Appendix C: Notes on the empirical method

1. Data

Territory changes. The table below describes the details of the changes in territory that took place in France since 1816.

Year	Territorial Changes
1861	Annexion of *departements* of Savoie and Haute-Savoie, and of *Comte* de Nice
1869	Franco-Prussian war: loss of Alsace-Lorraine
1914-	WWI: East of France, from Nord Pas-de-Calais to Vosges, is occupied by German military.
1919	At the end of WWI, Alsace-Lorraine is re-integrated to French territory
1939	WW2: Loss of Alsace-Lorraine
1943	WW2: Loss of Corsica
1945	Current territory: Alsace-Lorraine and Corsica are re-integrated to French territory

These changes in territory results in large changes in the population and death counts. This is illustrated below for population. It is unclear how to compute mortality in the year of the change. We compute it by using a weighted average of the population at the beginning and end of the year.

Migration. In the HMD cohort population counts are available. However, because of migrations, these counts cannot be used to derive a survival curve for a cohort. Because of net positive immigration occurring in France, the number of individuals in a given cohort can even increase from one year to the next. This is especially true at the end of the Algerian War. (e.g. the size of the female cohort born in 1910 increases from $300, 369$ to $303, 273$ between 1962 and 1963, despite a reported mortality rate of 0.5162. . The unit of analysis in our model of mortality is a country cohort, hence abstracts from migration. In our model the mortality rates coincide exactly with the slope of the survival curve. This is not true in the HMD. The population of the cohort melts natives and immigrants of the same age.

2. Computing the death rates, survival rates and life expectancy

Death rates. When taking our model to the data we target the most direct counterpart of our modeled cohort "mortality rate", which is computed as the number of individuals who died during a year, divided by the number of individuals alive at the beginning of the day. In typical life tables this number corresponds to what demographer call q_t, the probability of dying in a given year, and is conceptually distinct to the mortality rate, denoted by m_t. The main difference lies in adjusting the denominator — the size of the population. As more individuals die during the year the population needs to be adjusted to estimate the size of the remaining population exposed to the risk of death. Because our baseline model does not take this adjustment into account, we compute a direct counterpart of our theoretical object. Therefore, we compute the raw death rate in year t for a given cohort , q_t , as follows:

$$q_t = \frac{D_t}{N_t}$$

where D_t is the death count for year t from the HMD cohort table and N_t is the population on January 1st of year t. The HMD makes adjustments to compute a probability that is corrected for the fact that the data do not tract the same individuals over time, so the probability of dying is not correctly computed for a given cohort. The q we estimate with the raw counts is very similar to what is reported by the HMD except for

the first year of life and the last years of life as shown in Figure 6. This results in our under-estimating life expectancy somewhat.

Survival curves. We compute the survival curve recursively as follows. After initializing $S_0 = 100$, we iteratively compute:

$$S_t = S_{t-1} \times (1 - q_{t-1})$$

Life expectancy. Life Expectancy (LE) is an important statistics for the health profile of a given cohort. We compute LE as a way of comparing our model to the data in a parsimonious way. While we try to provide informative estimates of cohort life expectancy, we do not claim that their accuracy is comparable to demographic studies. Nevertheless, as we treat the series generated by our model in exactly the same manner as the data series, we obtain pairs of LE that are readily comparable.

4. Estimation routine

We compute our estimates using Matlab's canned *fminsearch* routine, a downhill simplex method, and Powell (1964)'s conjugate direction method. We first estimate the model using *fminsearch* until the objective function changes by less than 10^{-3} . The objective function is the sum of squared errors between the model's survival's curve and the one from the data. We then use these estimates as starting values for Powell's routine. Once Powell's routine converges, we use the estimated values from this procedure and implement *fminsearch* again until it converges. The total estimations on the UCLA computing cluster takes several hours. Still, the exact values of the final estimates for the time series parameters remain sensitive to the choice of the initial values.

5. Bootstrapping standard errors

Estimates from sample data come with standard errors. However, the mortality rates in the HMD are computed from birth certificates of the total population, not a sample of it. A typical cohort in our study counts $400,000$ individuals. As a results, the standard errors are negligible and therefore do not report them for the French cohorts.

In contrast, we do compute the standard errors for the monkey estimates as the data in that case consist of samples of one or two hundreds of individuals. One way of bootstrapping the standard errors it, given a series of mortality rates for a cohort, to view each sample of size N as a sequence of Bernoulli trials with varying success rates. Alternatively, one can view the survival curve of a population of size N as an $N \times 1$ vector of age at death. One can produce bootstrap estimates by drawing with replacement M subsamples of size S and compute the empirical survival curve.